AD-A078 271   NAVAL POSTGRADUATE SCHOOL   MONTEREY CA   F/G 20/11
TRANSVERSE OSCILLATIONS OF SMOOTH AND ROUGH CYLINDERS IN HARMON--ETC(U)
SEP 79   S OZKAYNAK

UNCLASSIFIED   NL

1 OF 1
ADA
078271

END
DATE
FILMED
1 -80
DDC

NAVAL POSTGRADUATE SCHOOL
Monterey, California

LEVEL

DDC
RECEIVED
DEC 18 1979
A

(9) Master's

THESIS

TRANSVERSE OSCILLATIONS OF SMOOTH
AND ROUGH CYLINDERS IN HARMONIC FLOW

by

Suleyman Ozkaynak

September 1979

Thesis Advisor: T. Sarpkaya

79 12 17 101

REPORT DOCUMENTATION PAGE		READ INSTRUCTIONS BEFORE COMPLETING FORM
1. REPORT NUMBER	2. GOVT ACCESSION NO.	3. RECIPIENT'S CATALOG NUMBER
4. TITLE (and Subtitle) Transverse Oscillations of Smooth and Rough Cylinders in Harmonic Flow		5. TYPE OF REPORT & PERIOD COVERED Engineer's and Master's Thesis; September 1979
		6. PERFORMING ORG. REPORT NUMBER
7. AUTHOR(s) Suleyman Ozkaynak		8. CONTRACT OR GRANT NUMBER(s)
9. PERFORMING ORGANIZATION NAME AND ADDRESS Naval Postgraduate School Monterey, California 93940		10. PROGRAM ELEMENT, PROJECT, TASK AREA & WORK UNIT NUMBERS
11. CONTROLLING OFFICE NAME AND ADDRESS Naval Postgraduate School Monterey, California 93940		12. REPORT DATE September 1979
		13. NUMBER OF PAGES 78
14. MONITORING AGENCY NAME & ADDRESS(if different from Controlling Office)		15. SECURITY CLASS. (of this report) Unclassified
		15a. DECLASSIFICATION/DOWNGRADING SCHEDULE

16. DISTRIBUTION STATEMENT (of this Report)

Approved for public release; distribution unlimited

17. DISTRIBUTION STATEMENT (of the abstract entered in Block 20, if different from Report)

18. SUPPLEMENTARY NOTES

19. KEY WORDS (Continue on reverse side if necessary and identify by block number)

Hydroelasticty
Strumming
Vortex-Induced Oscillations

20. ABSTRACT (Continue on reverse side if necessary and identify by block number)

   The dynamic response of elastically-mounted cylinders in a sinusoidally oscillating two-dimensional flow has been investigated both theoretically and experimentally.

   The experiments were carried out in a large U-shaped water tunnel, with smooth and sand-roughened circular cylinders. The results have been expressed in terms of lift coefficients, relative amplitudes of oscillation, Keulegan-Carpenter number, Reynolds number, Strouhal number, and a mass parameter. —> next page

DD FORM 1473 EDITION OF 1 NOV 68 IS OBSOLETE
1 JAN 73
(Page 1)   S/N 0102-014-6601

cont. A theoretical analysis has been carried out by assuming the transverse force varies harmonically. Furthermore, the instantaneous values of the displacement have been predicted through the use of the Duhamel's integral.

The results have shown that elastically-mounted cylinders undergo synchronous oscillations at a reduced velocity of 5.7 when the vortex shedding frequency coincides with the natural frequency of the cylinder. Away from the region of synchronization the cylinder is subjected to forced response by vortices shedding at a frequency smaller or larger than the natural frequency of the cylinder.

Accession For

NTIS C.A&I
DDC TAB
Unannounced
Justification

By
Distribution/
Availability Codes

Dist   Avail and/or
        special

A

TRANSVERSE OSCILLATIONS OF SMOOTH AND

ROUGH CYLINDERS IN HARMONIC FLOW

by

Suleyman Ozkaynak
Lieutenant, Turkish Navy
B.S., Naval Postgraduate School, 1978

Submitted in partial fulfillment of the
requirements for the degree of

MASTER OF SCIENCE IN MECHANICAL ENGINEERING

and the degree of

MECHANICAL ENGINEER

from the
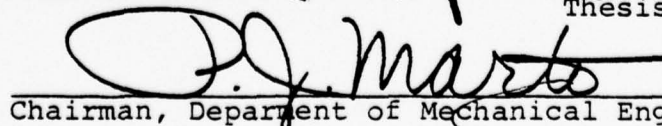
NAVAL POSTGRADUATE SCHOOL

September 1979

Author _____

Approved by: _____
Thesis Advisor

_____
Chairman, Department of Mechanical Engineering

_____
Dean of Science and Engineering

3

ABSTRACT

The dynamic response of elastically-mounted cylinders in a sinusoidally oscillating two-dimensional flow has been investigated both theoretically and experimentally.

The experiments were carried out in a large U-shaped water tunnel, with smooth and sand-roughened circular cylinders. The results have been expressed in terms of lift coefficients, relative amplitudes of oscillation, Keulegan-Carpenter number, Reynolds number, Strouhal number, and a mass parameter.

A theoretical analysis has been carried out by assuming the transverse force varies harmonically. Furthermore, the instantaneous values of the displacement have been predicted through the use of the Duhamel's integral.

The results have shown that elastically-mounted cylinders undergo synchronous oscillations at a reduced velocity of 5.7 when the vortex shedding frequency coincides with the natural frequency of the cylinder. Away from the region of synchronization the cylinder is subjected to forced response by vortices shedding at a frequency smaller or larger than the natural frequency of the cylinder.

TABLE OF CONTENTS

LIST OF FIGURES

NOMENCLATURE

A_1	Free surface displacement amplitude
A_m	Maximum amplitude of flow oscillation
B	Accelerometer output signal
C_{LM}	Maximum lift coefficient
C_{LM}^c	Calculated maximum lift coefficient
D	Cylinder diameter
$F_{1,2}$	Transverse forces measured at the cylinder ends
F_L	Fluid lift force
F_{LM}	Maximum fluid lift force
f_c	Frequency of cylinder oscillation (Hz)
f_n	Natural frequency (Hz)
f_{na}	Natural frequency in air (Hz)
f_{nw}	Natural frequency in water (Hz)
f_v	Vortex shedding frequency
g	Gravitational acceleration
H	Mean height of the free surface above the pressure taps
K	Keulegan-Carpenter number
k_s/D	Roughness ratio
k	Spring constant
L	Cylinder length
M	Mass
M_a	Added mass
p	Pressure
Re	Reynolds number ($Re = U_m D/\nu$)
r.m.s.	Root-mean-square

S	Sum of the force transducer outputs ($F_1 + F_2$)
St	Strouhal number ($St = f_v D / U_m$)
T	Fluid flow period
T_c	Cylinder oscillation period
T_v	Vortex shedding period
t	time
t_v	Duhamel superposition impulse time
U	Fluid flow velocity
U_m	Maximum fluid flow velocity
U_r	Reduced velocity ($U_m / f_n D$)
Y_M	Maximum cylinder displacement
$\bar{Y}_M$	Maximum normalized cylinder displacement (Y_M / D)
Y_o	Initial cylinder displacement
$\dot{Y}_o$	Initial cylinder velocity
y	Cylinder displacement
$\dot{y}$	Cylinder velocity
$\ddot{y}$	Cylinder acceleration
V	Velocity
Λ	Mass parameter ($\Lambda = \dfrac{M\zeta}{\rho D^2 L}$)
β	Frequency parameter ($\beta = D^2 / \nu T$)
ρ	Fluid density
θ	Vortex phase angle
ψ	Phase angle
ν	Kinematic viscosity
ω_n	Circular natural frequency (rad/sec)
ω_v	Circular vortex frequency (rad/sec)

ζ	Damping ratio
ζ_a	Damping ratio in air
ζ_w	Damping ratio in water

ACKNOWLEDGEMENT

The author would like to express his sincere appreciation to his advisor Professor T. Sarpkaya for his guidance throughout the investigation and for his help with the composition of the thesis.

In addition, the author wishes to acknowledge the help given by the personnel of the machine shop of the Department of Mechanical Engineering in constructing the test apparatus. In particular, I wish to thank Mr. Jack McKay for his superb workmanship.

I. INTRODUCTION

The investigation of the nonlinear deterministic or sta-
tistical response of an offshore structure or of its tubular
members is of considerable interest and may be carried out
through mathematical modeling, small-scale experiments, and
prototype testing or through a combination of these tech-
niques.

Much of what is known about the wave forces and moments
acting on bodies and complex structures of various shapes
came from field data and experiments in wave channels. To
extrapolate from these to the prediction of forces on new
structures in natural waves is often very uncertain, due to
the difficulty or impossibility of modeling all parameters
that might have an effect. For example, there is considerable
uncertainty as to how to account for the effect of currents
which may be superposed on waves $\angle^- 1 \_7$, for the elasticity
and flow induced oscillation of the members of the structure,
for the roughness and diametral increase of the connecting
members, for the effects of ambient flow with shear, etc.,
not to mention the two most commonly discussed dimensionless
parameters, namely, the Reynolds number and the relative
amplitude.

Studies of Reynolds number, relative amplitude, and
roughness effects on the in-line and transverse force coeffi-
cients have recently been carried out by Sarpkaya $\angle^- 2, 3 \_7$.

12

These studies were prompted by the need for systematic data and partly by the controversy concerning the influence of Reynolds number and surface roughness on the time-dependent loads on circular cylinders in harmonic flow. In all the experiments, the cylinders were mounted rigidly enough so that there was no possibility of either in-line and/or transverse oscillation.

The structural members in a prototype are seldom, if ever, designed to preclude the occurrence of forced or synchronized oscillations under the action of waves and/or currents. Evidently, the oscillating flow can cause vibrations in the in-line direction. More importantly, however, the transverse force, which is associated with vortex shedding, may give rise to serious transverse oscillations. The much-mentioned failure /‾4_/ of Texas Tower No. 4, an offshore platform off the coast of New Jersey, on 15 January 1961, is a classic example of vibration of a marine structure induced by oscillating flow and currents. It is evident from the foregoing that methods of prediction must be developed to prevent catastrophic flow-induced vibrations of the tubular members of marine structures subjected to wave action.

II. REVIEW OF PREVIOUS INVESTIGATIONS

The non-linear vibration problems of elastically-mounted
structures in oscillating flows have not been sufficiently
explored. While much progress has been made regarding the
in-line and transverse forces acting on stationary structures
$\underline{/}^{-}2$, $3\underline{/}$ and regarding the oscillations of elastic structures
in steady flows (see, e.g., Refs $\underline{/}^{-}5$-$7\underline{/}$.), there has been
relatively little theoretical and experimental work on the
complex dynamic response of elastic structures to oscillating
flows. This has been partly due to the lack of reliable data
for the force transverse-coefficients for both stationary and
vibrating structures.

Laird $\underline{/}^{-}8\underline{/}$ explored, in 1962, the effects of support
flexibility by oscillating a vertical cylinder through still
water. He found that the forces acting on a flexibly-supported
oscillating cylinder can exceed 4.5 times the drag force on
the cylinder rigidly-supported while moving at a uniform
velocity equal to the maximum velocity during the oscillation
and that a cylinder, flexible enough to have transverse oscil-
lations with amplitudes more than half the diameter, while
performing large amplitude oscillations in water, tends to
oscillate transversely at the eddy-shedding frequency and to
vibrate at twice the eddy frequency in the in-line direction.
Laird's work pointed out the significance of the vibrations
in harmonic flow and the need for a detailed investigation of
the phenomenon.

14

Vaicaitis $\underline{/\,^- 9\,\underline{/}}$ investigated the response of deep-water piles due to cross-flow forces generated by wind-induced ocean waves. The resulting cross-flow forces were treated as random processes in the time-space domain and were assumed to be dependent on fluid velocities and vortex shedding processes. Out of necessity, Vaicaitis had to make a number of assumptions regarding the structural motion, the added mass coefficient, Strouhal number, etc. Vaicaitis was careful to note that some of his conclusions were based on a particular example and that they might not be true for piles with different dynamic characteristics.

Selna and Cho $\underline{/\,^- 10\,\underline{/}}$ investigated the in-line resonant response of a tall structure by assuming constant drag and inertia coefficients in calculating the exciting fluid force through Morison's equation $\underline{/\,^- 11\,\underline{/}}$, modified to take into account the motion of the structure. Their calculations have shown that a resonant motion is possible and that the dynamic deflection of a flexible structure can considerably exceed its static deflection.

Verly and Every $\underline{/\,^- 12\,\underline{/}}$ measured wave-induced stress on similar rigid and flexible vertical cylinders in a wave channel at relatively low Keulegan-Carpenter and Reynolds numbers. Even though they were unable to correlate their data with any suitable parameter governing the motion, they concluded that the vibration is caused by the cylinder's response to eddy shedding and that there is no fluid-structure interaction. They found that the vibration occurs if $U_m / f_n D$

15

(U_m represents the maximum velocity of flow or wave in a cycle; and D, the diameter of the cylinder) is greater than about unity for any natural frequency, wave frequency, and damping. The U_m/f_nD parameter never reached high enough values in Verly and Every's experiments for the cylinder to undergo synchronized oscillations as the present investigation has shown.

McConnell and Wilson $\underline{/}13\underline{}\underline{7}$ conducted experiments similar to those of Laird $\underline{/}8\underline{}\underline{7}$ by sinusoidally driving a circular cylinder in still water. These experiments were conducted at rather small Reynolds numbers (Re = U_mD/ν) with 0.25 in and 0.50 in cylinders. Furthermore, these investigators measured only the amplitude of oscillation and calculated the lift coefficient at resonance from a slightly-modified version of an equation developed by Sarpkaya $\underline{/}14\underline{}\underline{7}$. They have concluded that U_m/f_nD is one of the most important parameters governing the resonant oscillations.

Sawaragi et al. $\underline{/}15\underline{}\underline{7}$ investigated the in-line and transverse dynamic response of a cantilevered circular cylinder, with a concentrated mass at its top, in waves of small amplitude. The Reynolds number ranged from 1,500 to 6,200 and the rms value of the Keulegan-Carpenter number (calculated over the submerged length of the cylinder through the use of rms value of the maximum of the horizontal velocities) ranged from 2 to about 20. They have approximated the lift coefficient for a rigid cylinder by a Rayleigh distribution and calculated the dynamic response of the test cylinder. The

16

results are of limited value since the interaction between the synchronization and the force amplification was ignored and since no more than three vortices were shed during a half cycle. Furthermore, the rapid variation of the Reynolds number, Keulegan-Carpenter number, vortex-shedding coherence, and lift force with depth, in a range of Keulegan-Carpenter numbers where the phenomenon is least understood, obscured the role played by the governing parameters.

It is clear from the foregoing that there are no well-established analytical methods either to analyze the data or to predict the characteristics of the flow or of the vibration. Thus, it was decided to undertake a comprehensive investigation of the dynamic response of elastically-mounted smooth and rough cylinders in harmonic flow particularly at high Reynolds numbers and Keulegan-Carpenter numbers.

III. EXPERIMENTAL EQUIPMENT AND PROCEDURES

A. U-SHAPED OSCILLATING-FLOW TUNNEL

The equipment used to generate the harmonically oscilla-
ting flow has been extensively used at this facility over the
past six years $\underline{/}$ 2 $\underline{/}$, $\underline{/}$ 3 $\underline{/}$. Only the salient features, most
recent modifications, as well as the adaptation for this work,
are briefly described in the following.

The length of the U-shaped vertical water tunnel has been
increased from 30 ft to 35 ft and its height from 16 ft to 24
ft. Previously, a butterfly valve arrangement at the top of
one of the legs was used to initiate the oscillations. During
the past year, the tunnel has been modified so that oscilla-
tions can be generated and maintained indefinitely at the
desired amplitude. For this purpose the output of a 2 Hp fan
was connected to the top of one of the legs of the tunnel with
a large pipe. A small butterfly valve, placed in a special
housing between the top of the tunnel and the supply line,
oscillated harmonically at a frequency equal to the natural
frequency of the oscillations in the tunnel. The oscillation
of the valve was perfectly synchronized with that of the flow
through the use of a feedback control system. The output of
a pressure transducer (sensing the instantaneous acceleration
of the flow) was connected to an electronic speed-control unit
coupled to a DC motor oscillating the valve plate within 0.001
seconds. The amplitude of oscillations was varied by

constructing or enlarging an orifice at the exit of the fan. The flow oscillated at a given amplitude as long as desired.

Smooth and sand-roughened aluminum cylinders of 4 in diameter were used in the experiments. Each cylinder was rigidly fixed to two load cells and the low-friction linear bearings mounted on two matched helical springs.

B. CYLINDER SUPPORTS AND HOUSINGS

Initially, beam springs were considered for the elastic cylinder supports. However, the requirements for rigidity, strength and torsional stability in the in-line direction quickly led to the use of helical steel springs. In the formal design, the cylinder was rigidly fixed to two low-friction linear bearings resting on two matched helical springs. The motion of the bearings was constrained by two rods perpendicular to the direction of the flow as shown in Fig. 1. Detailed drawings of the system are shown in Figs. 2, 3, and 4.

The force transducers had a capacity of 500 lbs with an overload capacity of 200 percent. The transducers were mounted as shown in Fig. 4 to the aluminum split-bearing housing blocks. Each block was manufactured to accommodate an adjustable ball bushing with a nominal 2.5 in bore and a length of 5 in. The bearings rode on 2.5 in diameter stainless steel, hardened and ground, solid shafts. Adjustments of the bearing diameter eliminated bearing chatter. The springs were centered around the shafts by a retaining ring on the housing and by the yoke support at the bottom.

19

The yoke supports allowed the blocks and springs to be raised or lowered to center the cylinders vertically in the test section and permitted the use of various cylinders, springs and weights while accommodating the effects of the buoyant force. Each yoke was positioned by brass rods suspended through the top of the housing by another yoke which was positioned with precision by a threaded third brass rod passing through the upper yoke and lifting against the housing top. Alignment of mounts and rods was accomplished by a jig which was placed between the two blocks, leveled, then raised, and lowered to position the two stainless steel rods.

Figure 5 shows a dimensioned drawing of one of the two support housings. Each was welded of 3/8 in aluminum plate. The windows were covered by removable plexiglass plates for access for calibration and maintenance, or, when mounted in place, for the observation of cylinder movement during tunnel operation. Vents and drains were installed at top and bottom of the housing to remove air or water in filling or draining. The housings were flanged and bolted to the U-tunnel wall with O-ring seals for water proofing as may be seen in Fig. 3.

Linear-variable-displacement transducers (LVDT) were installed between each bearing block and housing. Each LVDT was energized by a six volt DC regulated power supply. The LVDT's provided displacement from the equilibrium position and also helped to verify the simultaneous and in-phase vertical oscillation of both ends of the cylinder.

The circular cylinder models used for this study were turned
on a lathe from aluminum pipes and polished to a mirror shine.
The length of each cylinder was such as to allow 1/32 in
clearance between the tunnel wall and each end. As part of the
total length, smooth circular flanges 6.0 in diameter and 1/8 in
thick were attached to the ends of the cylinder to eliminate
the end effects.

All cylinders were hollow, and each contained a beam type
accelerometer. Figure 6 shows a cutaway drawing of a cylinder
with the accelerometer installed in the exact center of the
cylinder. The electrical connection to the accelerometer is
led through a notch in the male fitting at the end of the
cylinder. Sealing of the unit is accomplished by O-rings and
threaded fittings.

A 6.0 in circular access hole was cut in the tunnel walls
at the test section. Each hole was covered with a plate of
identical size. A slot of 1.0 in by 5.0 in was cut in each
cover. The covers allowed the installation of the cylinders,
and the slots allowed the unobstructed linear oscillation of
the force-transducer arms attached to the cylinder.

C. MEASUREMENT OF BASIC PARAMETERS

For the determination of k, a known weight was suspended
from the center of the cylinder, and the displacement was
measured. The natural frequency in air, f_{na}, and the natural
frequency in water, f_{nw}, were determined by plucking the
cylinder and allowing it to oscillate freely in the particular
fluid medium. The displacement was recorded on one channel

21

recorder. A sample trace is shown in Fig. 7. Along with the frequencies, the logarithmic decrement and the damping factors, ζ_a, and, ζ_w, were determined in air and water, respectively.

The mass, M, of the system was then calculated from

$$M = k \, / (2\pi f_{na})^2 \qquad\qquad (1)$$

and the added mass of the system was determined from

$$M_a + M = k/(2\pi f_{nw})^2 = M(f_{na}/f_{nw})^2 \qquad\qquad (2)$$

For the purpose of verification of the measured values, M_a for the cylinder was computed through the use of the observed values of frequencies and found to be within one tenth of one percent of that given by the potential flow theory and independent experiments.*

A trace was also made of the output of the accelerometer oscillating in free vibration. The frequency of this device was found to be 44.5 Hz with a damping factor of $\zeta = 0.0022$. According to Thompson $/\overline{}16\_7$, for frequencies up to 5 Hz this accelerometer would provide true force readings with a magnification factor nearly equal to unity. The frequency of oscillation in the present investigation ranged from 1.5 Hz to 4.0 Hz.

---

* The theoretical value of the added mass coefficient for a circular cylinder is equal to 1.0.

Amplitude, acceleration, elevation or velocity of the fluid was a matter of interpretation of the signal received from the same instrument. In this experiment use was made of a differential pressure transducer with pressure taps located on the two legs of the tunnel. Knowing the height of the mean water level above the taps, H, the above values were solved for by application of Bernoulli's equation. For example, the virtual amplitude is given by $/\overline{}2\_7$

$$A_m = 2A_1 = \frac{\Delta P}{1 - \frac{1}{g}(2\pi/T)^2 H} \qquad (3)$$

in which the gravitational acceleration, g, and the period of flow oscillation, T, remain constant.

By examination of the free body diagram shown in Fig. 8, it is seen that the only transverse forces acting on the cylinder are those reaction forces from the two transducers, the fluid force and the product of the cylinder mass and acceleration. Therefore, the fluid force is given by

$$F_L = F_1 + F_2 - M\ddot{y} \qquad (4)$$

The sensitivity of the accelerometer was adjusted to yield $F_L = 0$ while the cylinder freely oscillated in air. This

23

method allowed the measurement of the net fluid force with an error less than 1.5 percent.

D. ELECTRONIC CIRCUITRY

The output of each of the two LVDT's, after amplification by a low-gain amplifier, was displayed on an eight-channel recorder as in Fig. 9. One of the two signals was additionally displayed on a three-channel recorder.

The output of the force transducers was separately amplified by a carrier amplifier, filtered by a Krohn-Hite electronic filter and displayed on the eight-channel recorder. Then the two signals were added together by an electronic summing circuit, amplified again by a low level preamplifier and displayed on the eight-channel recorder.

The accelerometer output was similarly amplified by a carrier amplifier and filtered by a low pass filter. This signal was also displayed on the eight-channel recorder. It was then subtracted from the sum of the force signals through the use of a summing-differencing electronic circuit. This resultant signal, representing the fluid force on the cylinder, F_L , was again amplified by a low level preamplifier and displayed on both the three- and eight-channel recorders. Figure 10 is a block diagram of the circuits described above.

The signal from the differential pressure transducer was of such quality that it did not require any filtering. As shown in Fig. 11, it was amplified by a carrier amplifier and displayed on the two aforementioned recorders.

24

E.   PROCEDURES

Procedures for a series of runs were as follows:

1.   The cylinder was aligned with the tunnel by adjusting the bearings. The sensitivities of the force transducers were matched by hanging a known weight from the exact center of the cylinder. At the same time a calibration factor was determined by measuring the displacement and comparing it with the output of the LVDT of the three-channel recorder.

2.   The accelerometer was calibrated by plucking the cylinder (quickly releasing the cylinder from a displaced position and allowing it to oscillate freely) and adjusting the amplifier gain until the fluid force in the air was nulled to within 1.5 percent deviation.

3. f_{na} and ζ_a were also determined by plucking the cylinder in air.

4.   The weight was then suspended from the cylinder center, this time for the measurement of a calibration factor in lbf/mm of the three-channel-recorder output at a particular gain setting.

5.   The U-tunnel and cylinder-support housings were again filled to the top of the test section, and all air was vented from the housings.

6.   The cylinder was then lowered to the center of the test section by simultaneously lowering both sets of spring yokes, each the same number of turns, to compensate for the buoyant force on the displaced cylinder.

7.   The cylinder was plucked, and f_{nw} and ζ_w were calculated from the free-oscillation traces.

25

8. The access to the horizontal test section above the cylinder, through which the weights were lowered to the cylinder, was closed. The tunnel was filled with water from a sump tank located near the apparatus. Filling was accelerated by a large submerged sump pump.

9. The differential-pressure transducer was bled of any entrained air and its calibration verified.

10. The tunnel oscillations were started by actuating the control system and the blower.

11. The amplitude of flow oscillations were set at a desired value and the forces, displacements, and flow acceleration were recorded simultaneously.

12. Three or more runs were made at a paper speed of 25 mm/sec at each combination of spring, cylinder and flow amplitude.

13. At the end of each set of runs, f_{nw} and ζ_w were measured to verify the initial values before draining the tunnel.

Two additional runs were made with the cylinder mounts fixed to verify the results previously obtained by Sarpkaya $\underline{/}2\underline{/}$. The force transducers were turned 90 degrees and pinned to measure the in-line forces. Also readings of these forces were taken with the cylinder free to oscillate. Data from these runs proved to be as expected, and they were not repeated for the larger cylinder.

F. DATA REDUCTION

Test runs were selected for evaluation on the basis of oscillation amplitude, Reynolds number, and Keulegan-Carpenter number. For each run evaluated, the peak lift force, F_{LM} ; peak displacement, Y_M ; shortest force- and displacement-periods, T_V and T_C ; and flow amplitude were recorded for each half cycle of flow oscillation. Also recorded was such relevant information as calibration factors, cylinder diameters, gain settings, k, ζ_w . f_{nw} , etc. A computer program calculated the peak lift coefficient, C_{LM} , as follows:

$$C_{LM} = \frac{F_{LM}}{\frac{1}{2} \rho U_m^2 LD} \tag{5}$$

where ρ is the density of the fluid; and L , the length of the cylinder. Other variables computed included: A_m , U_m , K , Y_M/D , $U_m/f_n D$, and the Strouhal number St.

27

IV. ANALYSIS

The amplitudes of the lift coefficient and the relative displacement may be shown to be governed by

$$\{C_{LM}, Y_M/D\} = f_i \{U_m T/D, D^2/\nu T, U_m/f_{n\omega}D, k_s/D, \zeta_a, M/\rho LD^2\} \quad (6)$$

where

$$C_{LM} = F_{LM}/(0.5\rho LDU_m^2) \quad (7)$$

and U_m represents the amplitude of velocity oscillations; f_{nw}, the in-water natural frequency of the oscillating system; D, the diameter of the cylinder; ν, the kinematic viscosity; T, the period of the flow oscillations; k_s, the roughness height, ζ_a, the damping ratio in air; M, the mass of the oscillating system; ρ, the density of the fluid; and L, the length of the cylinder. The last two parameters in Eq. (6) may be combined as $M\zeta_a/(\rho LD^2)$ on the basis of experience with hydroelastic oscillations in steady flow $\underline{/^-7\_/}$.

The lift coefficient and the Strouhal number for a non-oscillating cylinder are governed by

$$\{S^0, C_{LM}^0\} = g_i \{U_m T/D, D^2/\nu T, k_s/D\} \quad (8)$$

In fact, the three parameters in Eq. (8) determine uniquely all the characteristics of the base flow. Missing from the above relationship is the effect of the correlation length. For smooth circular cylinders the lock-in or the forced-oscillatory motion is accompanied by increased coherence in the shedding along the body. This increased correlation was thought to be primarily responsible in increasing the force and hence the amplitude to some limit set by the flow. Experiments with bodies with fixed seperation lines (and suitable after body) have shown $\underline{/}$ 17 $\underline{/}$ that the increase in correlation length can account for only a small fraction of the large increase in the transverse force near lock-in. The fluid response to the body motion or the interaction between the fluid motion and the body motion is the primary reason for the lock-in and the increase in the transverse force.

The problem under consideration requires the solution of the separated, time dependent flow about an oscillating cylinder. Such a solution is hard to come by in view of the fact that a solution does not exist even for steady flow about a cylinder at rest. Thus, a phenomenologically based analysis coupled with experimental observations is the best one can perform at present. Hopefully, the insight gained through such an analysis will eventually lead to the formulation of an heuristic model.

The equation of motion for an elastically-mounted rigid cylinder of mass M, damping coefficient ζ, circular natural frequency ω_n, and spring constant k, is given by

$$M\ddot{y} + 2M\zeta\omega_n\dot{y} + ky = F(t) \tag{9}$$

where y represents the transverse displacement of the cylinder and F(t) the exciting force or the lift force. In general F(t) depends on the parameters given by Eq. (6) or simply $U_r = U_m/f_n D$ and $M\zeta/(\rho LD^2)$. For sake of simplicity, F(t) may be assumed to be given by

$$F(t) = 0.5\rho LDU_m^2 \, C_{LM} \, \sin(\omega_v t + \theta) \tag{10}$$

in which $\omega_v = 2\pi f_v$ and θ is the phase angle. However, even during the period of nearly perfect synchronization, the lift force does not retain a constant amplitude and frequency. Furthermore, the velocity U varies as $U = U_m \sin 2\pi t/T$ during a given cycle. In general, it is necessary to consider the harmonics of the lift force together with their spectral energy. Prior to such a detailed analysis, it will be hypothesized and subsequently verified by the present results that the rate of energy transfer from the fluid to the oscillating body is proportional to the rms value of the velocity.

Writing,

$$\frac{1}{T}\int_0^T U^2 \, dt = \frac{1}{T}\int_0^T U_m^2 \, \sin^2 2\pi f_n t \, dt = \frac{U_m^2}{2} \tag{11}$$

and combining with Eq. (10), one has

$$F(t) = \frac{1}{4}\rho LDU_m^2 \, C_{LM} \, \sin(\omega_v t + \theta) \tag{12}$$

30

The equation of motion may be written as

$$M\ddot{y} + c\dot{y} + ky = F_{LM}\sin(\omega_v t + \theta) \tag{13}$$

The steady state solution of this equation is given by

$$y = A \sin(\omega_v t + \theta) + B \cos(\omega_v t + \theta) \tag{14}$$

Substituting Eq. (14) in Eq. (13) and solving for A and B one has

$$A = F_{LM} \frac{(k - M\omega_v^2)}{(k - M\omega_v^2)^2 + \omega_v^2 c^2} \tag{15}$$

and

$$B = F_{LM} \frac{\omega_v c}{(k - M\omega_v^2)^2 + \omega_v^2 c^2} \tag{16}$$

Then, Eq. (14) may be written as

$$y = Y_M \cos\{(\omega_v t + \theta) - \psi\} \tag{17}$$

in which

$$Y_M = \sqrt{A^2 + B^2} \tag{18}$$

31

and

$$\psi = \tan^{-1} \left[\frac{2\zeta \frac{\omega_v}{\omega_n}}{1 - (\frac{\omega_v}{\omega_n})^2} \right] \qquad (19)$$

and

$$Y_M = \frac{F_{LM}/k}{\sqrt{\{1 - (\frac{\omega_v}{\omega_n})^2\}^2 + (2\zeta\frac{\omega_v}{\omega_n})^2}} \qquad (20)$$

then Eq. (17) reduces to

$$y = \frac{F_{LM}/k}{\sqrt{\{1 - (\frac{\omega_v}{\omega_n})^2\}^2 + (2\zeta\frac{\omega_v}{\omega_n})^2}} \cos (\omega_v t + \theta - \psi) \qquad (21)$$

Noting that $k = M(2\pi f_n)^2$, Eq. (20) reduces to

$$\overline{Y}_M = \frac{Y_M}{D} = \frac{(U_m/f_n D)^2 \ C_{LM} \ \rho L D^2}{16\pi^2 M \sqrt{\{1 - (\frac{\omega_v}{\omega_n})^2\}^2 + (2\zeta\frac{\omega_v}{\omega_n})^2}} \qquad (22)$$

At resonance $\omega_v \approx \omega_n$, and Eq. (22) becomes

$$\overline{Y}_M = \frac{Y_M}{D} = \frac{(U_m/f_n D)^2 \ C_{LM}}{32\pi^2 M \zeta / \rho L D^2} \qquad (23)$$

32

Equation (22) may also be written as

$$C_{LM} = \frac{\overline{Y}_M \left[16\pi^2 M \sqrt{\{1 - (\frac{\omega_v}{\omega_n})^2\}^2 + (2\zeta\frac{\omega_v}{\omega_n})^2} \right]}{\rho LD^2 (U_m/f_n D)} \qquad (24)$$

The above equation is used to compare the measured and calculated values of the lift coefficient in terms of the known and measured parameters appearing on the right-hand side of the equation.

The foregoing comparisons between the measured and calculated values of Y_M/D and C_{LM} are only for the peak values of the said parameters. Evidently, it is equally important to compare the evolution of the displacement as a function of time using the measured force as the input function.

Among the various techniques commonly used in the vibration analysis, Duhamel's superposition principle enables one to predict the displacement of a linearly-damped and elastically-mounted cylinder through the use of the following integral $\angle\overline{16}\angle$.

$$y = (Y_o - \frac{1}{M\omega_n} \int_o^t \frac{F(t) e^{-\zeta\omega_n(t-t_v)}}{\sqrt{1 - \zeta^2}} \sin\sqrt{1-\zeta}\, \omega_n t_v dt_v) \cos\omega_n t$$

$$+ (\frac{\dot{Y}_o}{\omega_n} + \frac{1}{M\omega_n} \int_o^t \frac{F(t) e^{-\zeta\omega_n(t-t_v)}}{\sqrt{1 - \zeta^2}} \cos\sqrt{1-\zeta}\, \omega_n t_v dt_v) \sin\omega_n t \qquad (25)$$

Equation (25) is used to compare the predicted and measured relative displacements for a series of selected runs.

V. DISCUSSION OF RESULTS

The results will be discussed first in terms of the maximum values of the lift coefficient and the amplitude of oscillation.

Figures 12 through 14 show the variation of C_{LM} with respect to the Keulegan-Carpenter number. The variation of the same parameter with respect to the reduced velocity U_r is shown in Figures 15 through 17 for a smooth cylinder and for a rough cylinder with two different damping parameters. All of these figures show that C_{LM} decreases rapidly with increasing K and U_r. Furthermore, C_{LM} is considerably larger for the rough cylinder. The change in damping does not change the value of C_{LM} as evidenced by a comparison of Figures 13 and 14 and of Figures 16 and 17. The smooth cylinder has not been tested with different damping ratios. However, it is expected that the data shown in Figures 12 and 15 will not vary with damping.

The variation of C_{LM} with the ratio of the vortex shedding frequency to the cylinder oscillation frequency is shown in Figures 18 and 19 for a smooth and a rough cylinder. Evidently, as vortex shedding frequency becomes nearly equal the cylinder oscillation frequency, the lift coefficient increases dramatically. It is this particular nature of the vortex-induced oscillations that has been referred to in the literature as self-excitation. A vortex-excited oscillation is actually a

34

forced one having a self-excited character also to some degree due to lift-force amplification through nonlinear interactions. By definition, self-excited oscillation is one where the alternating force that sustains the motion is created or controlled by the motion itself; when the motion stops, the alternating force disappears. For the phenomenon discussed herein the alternating lift force does not disappear when there is no oscillation. In fact, when there is no alternating force (a flat plate normal to the flow) there is no lock-in. Apparently, the often-used definition of "self-excited oscillation" is a misnomer.

The calculated values of C_{LM} in the synchronization region, through the use of Eq. (24) and the measured values of Y_M/D and ζ, are compared with those measured directly in Figure 20. Clearly, the measured and predicted values are in good agreements in the region where Eq. (24) is valid. In reality, a number of frequencies exists for the vortex shedding even in the synchronization region ($0.95 < f_v/f_n < 1.05$). This is particularly true for smooth cylinders where the vortex shedding along the cylinder is not well correlated. For rough cylinders the correlation along the length of the cylinder is almost perfect $\underline{/}2\underline{\,/}$. This is partly the reason for the better agreement between the measured and calculated values of C_{LM} shown in Figure 20.

The relative displacement of the cylinder is examined for both smooth and rough cylinders in terms of the reduced velocity, Keulegan-Carpenter number and the Reynolds number.

Figures 21 through 23 show the variation of Y_M/D as a function of U_r. The maximum amplitude at synchronization is reached at about $U_r = 5.9$ for the smooth cylinder and at about $U_r = 5.6$ for the rough cylinders. Experiments with steady flow about a tranversely-oscillating smooth cylinder have shown that $\underline{/7\_/}$ perfect synchronization takes place for U_r values between 5 and 7. Evidently, synchronization in harmonically oscillating flows falls in the lower range of U_r values just cited.

The variation of Y_M/D with the Keulegan-Carpenter number is shown in Figures 24 through 26. Apparently, the synchronization for the 4 in cylinder occurs at a Keulegan-Carpenter number of about 50. This result is not unexpected as will be demonstrated below.

The Strouhal number for a harmonically oscillating flow may be written as

$$St = \frac{f_v \, D}{U_m} \tag{28}$$

multiplying and dividing the right-hand side of this equation with T (the period of oscillations of the water in the tunnel) one has

$$St = \frac{f_v \, T}{K} \tag{29}$$

at synchronization f_v is nearly equal to f_n. For the 4 in cylinder $f_n = 1.6$ and $T = 6.$ sec. With an average Strouhal

36

number of 0.2 Eq. (29) yields K = 48 which compares quite well with the K value obtained from Figures 24-26.

The variation of Y_M/D with the Reynolds number is shown in Figures 27 through 29. For the particular cylinder the synchronization occurs at a Reynolds number about 100,000. A comparison of Figures 24-26 with 27-29 shows that the dependence of Y_M/D on K is exactly the same as that of Y_M/D on the Reynolds number. Even though, experiments have not been performed at a given K for different Reynolds numbers the results with steady flow experiments show that $\underline{/}\bar{7}\underline{/}$ Y_M/D at the synchronization does not depend on the Reynolds number in the range of Reynolds numbers from about 1,000 to 10^6 $\underline{/}\bar{7}\underline{/}$. Thus, Figures 27-29 actually reflect the variation of Y_M/D with the Keulegan-Carpenter number.

The amplification factor, defined by $Y_M k/F_{LM}$, in the synchronization region is plotted in Figures 30-32 as a function of f_v/f_n for both smooth and rough cylinders. Considering the difficulty of establishing and maintaining synchronization, the experimental results are in excellent agreement with that predicted by Eq. (20).

As noted earlier, synchronization is possible only when the frequency of the exciting lift force is close to the natural frequency of the oscillating system. Consequently, the Strouhal number plays a major role in the phenomenon. Figures 33 through 35 show the variations of Y_M/D and St with U_r. For the smooth cylinder the Strouhal number decreases from 0.2 to about 0.16 as one approaches synchronization.

37

Thereafter, the Strouhal number gradually increases to about 0.2. The variation of the vortex shedding frequency and hence the Strouhal number for smooth cylinders is strongly effected by the change of the correlation length $\underline{/}7\underline{\,/}$. On the other hand, roughness provides perfect correlation and Strouhal number remains nearly constant at St ~ 0.2 as seen in Figures 34 and 35. Apparently, roughness enables one to eliminate from consideration the effect of the correlation length. Initially experiments were conducted with a smooth cylinder. It was supposed that roughness will complicate the matters further. Contrary to this supposition, roughness and the harmonic nature of the flow further delineated the most important parameters governing the hydroelastic oscillations of cylinders.

Finally, Figure 36 shows the comparison of the instantaneous values of the measured cylinder displacement with those predicted through the use of the Duhamel's integral $\underline{/}$ see Eq. (27) $\underline{\,/}$. The measured force and other physical characteristics of the oscillating system (damping, mass and natural frequency) were used as input in the Duhamel's integral. The close agreement between the measured and calculated displacements is not surprising. It simply proves that the various parameters such as mass, damping ratio, displacement, etc., have been properly measured.

38

VI. CONCLUSIONS

The theoretical and experimental investigation of the hydroelastic oscillations of a smooth and rough circular cylinder in harmonic flow warranted the following conclusions:

1. An elastically-mounted cylinder may undergo synchronized oscillations when the reduced velocity $U_r = U_m/f_n D$ is equal to about 5.7.

2. The synchronized oscillations for a smooth cylinder occur at an average Strouhal number of about 0.16. The Strouhal number for the rough cylinder remains constant at a value of about 0.2.

3. In the region of synchronous oscillations, the lift coefficient is amplified by a factor of about 2 relative to that for a fixed cylinder in the same flow.

4. The analysis relating the governing parameters predicts fairly accurately the maximum amplitude of the oscillations for both the smooth and the rough cylinders in the synchronous region.

5. The measured instantaneous values of the cylinder displacement are in excellent agreement with those predicted through the use of the Duhamel's integral.

TOP VIEW

TEST CYLINDER

FORCE TRANSDUCER

SIDE VIEW

TEST CYLINDER

HELICAL SPRING

BEARING BLOCK
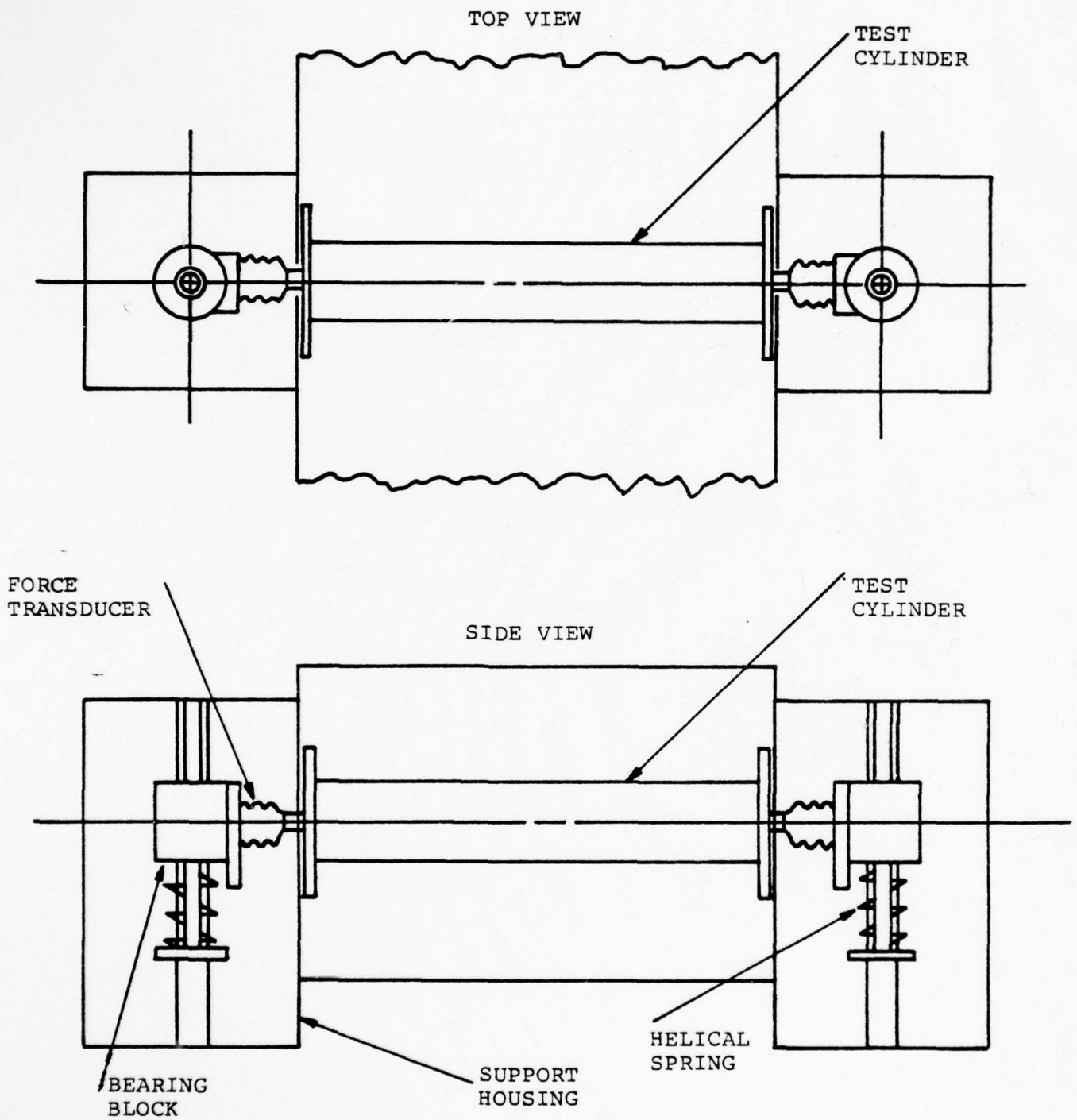
SUPPORT HOUSING

Fig. 1   Preliminary sketch of the supports and housings.
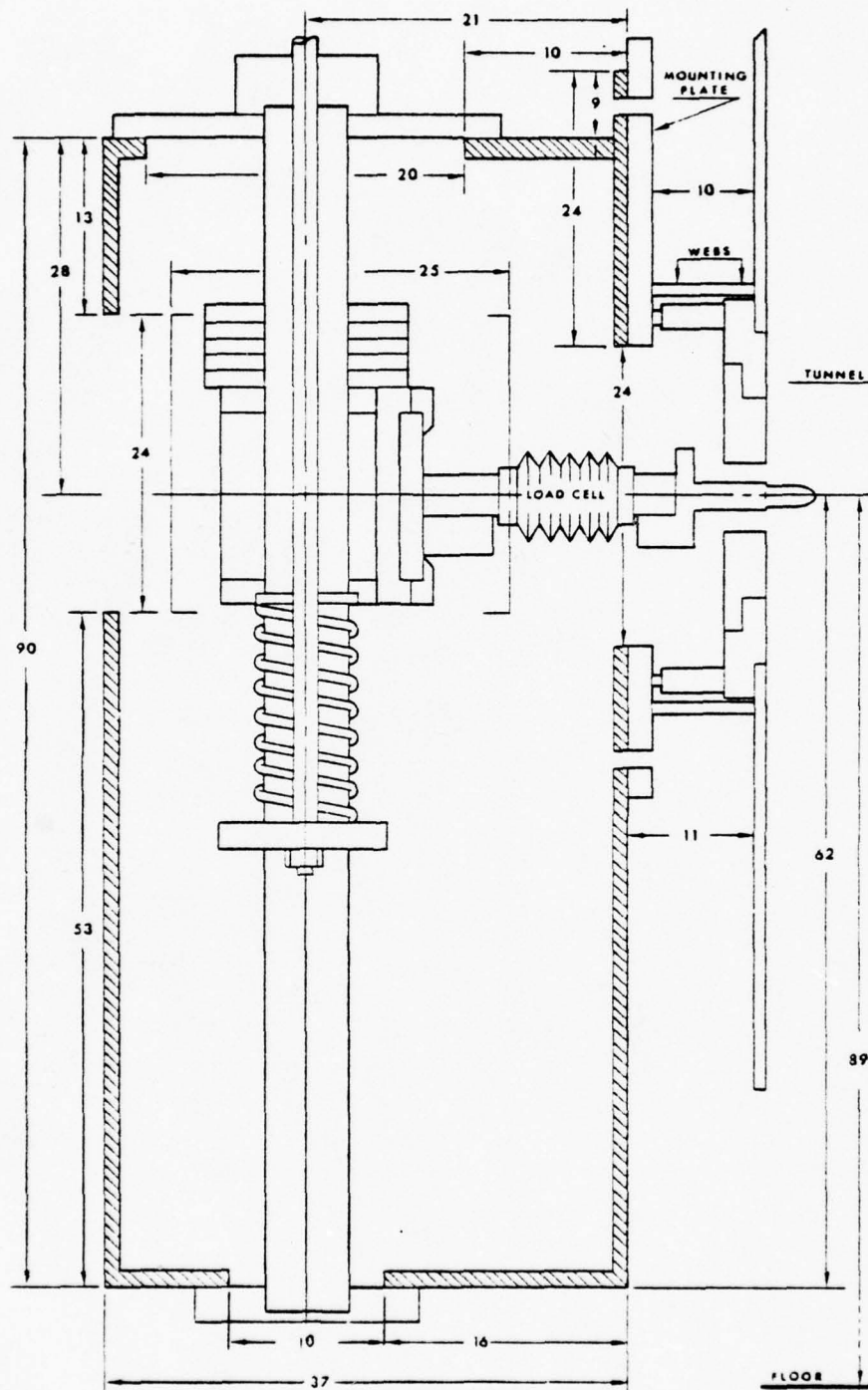
Fig. 2 Side view of a cylinder-support mount
and housings. (Dimensions in cm).

41
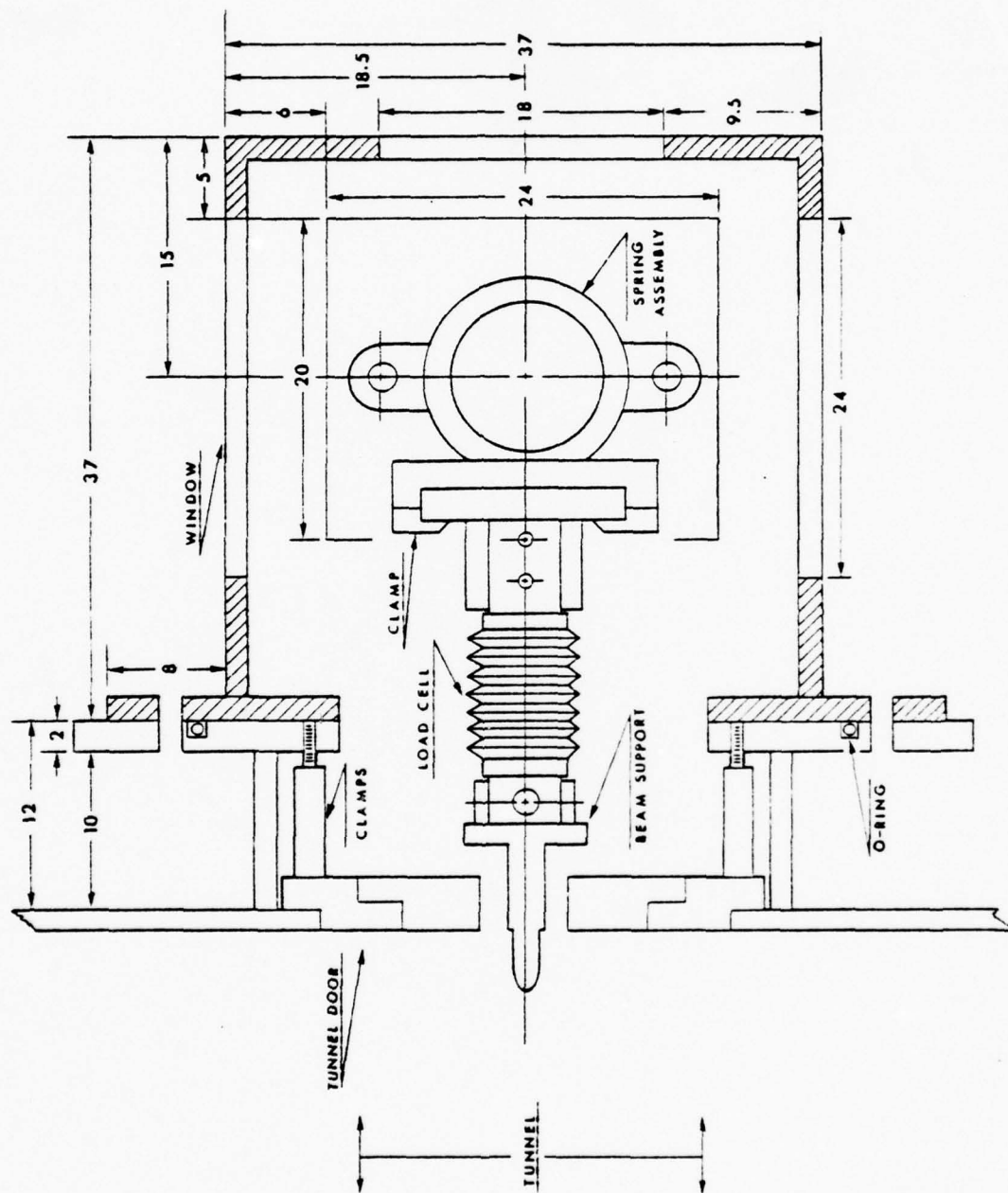
Fig. 3 Top view of a cylinder-support mount and housing. (Dimensions in cm).

42
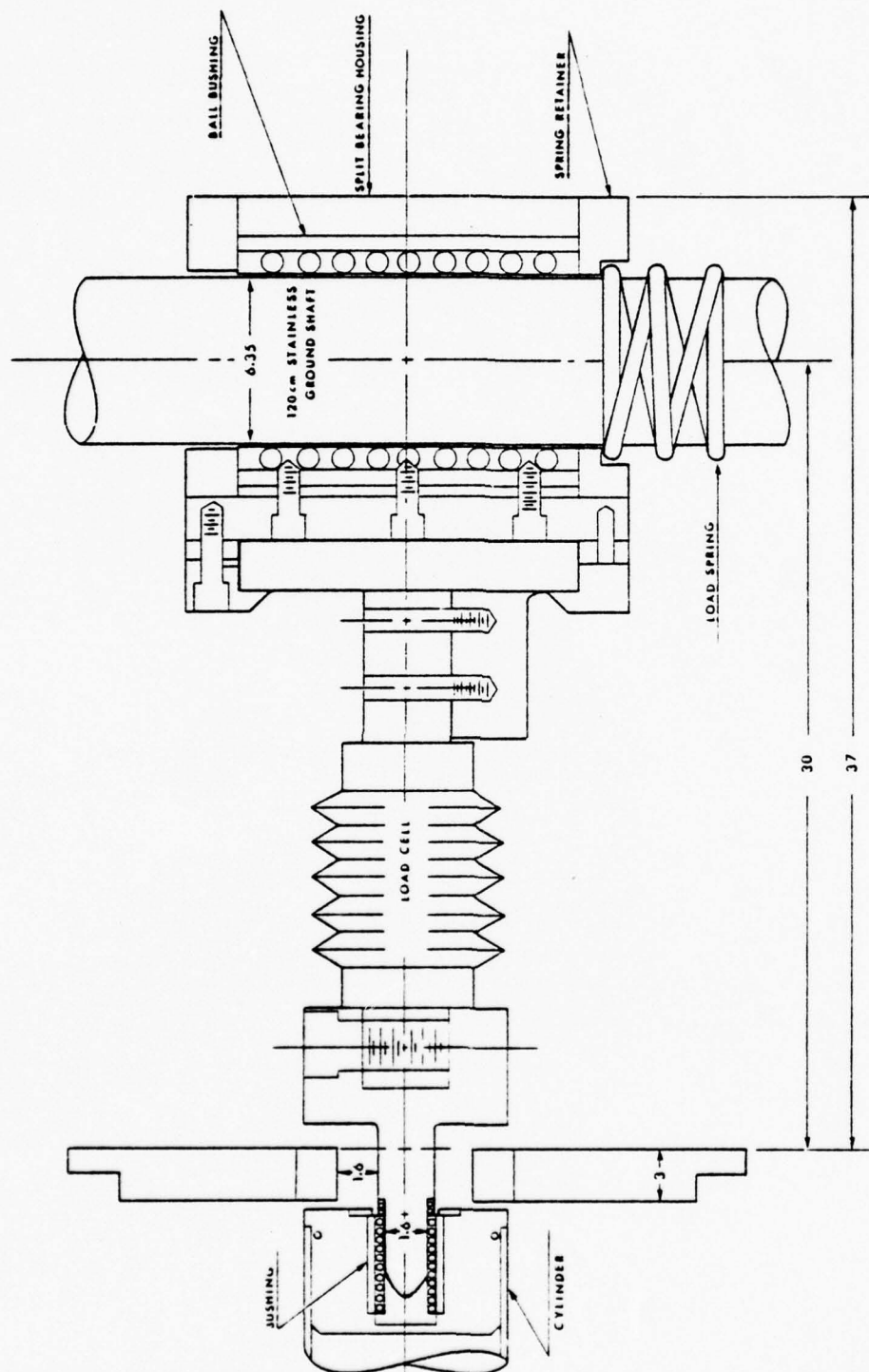
Fig. 4 Side Cutaway view of a Load cell and
bearing housing. (Dimensions in cm).
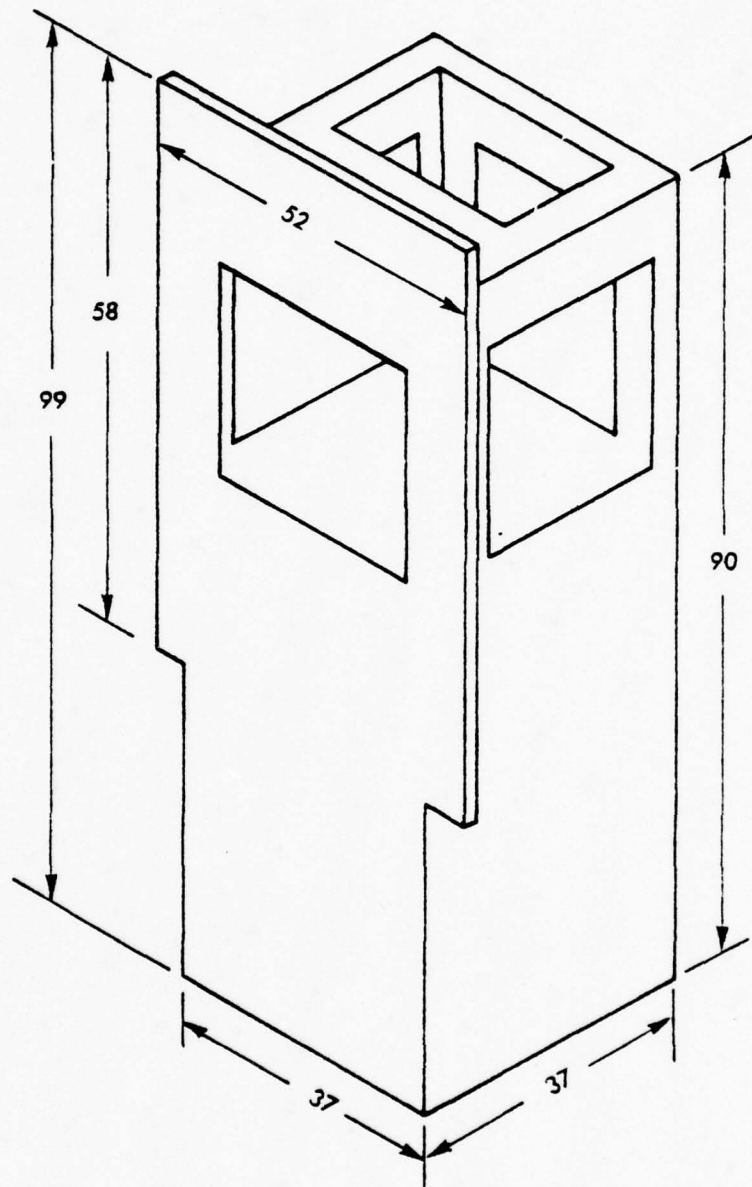
Fig. 5 Support housing.
(Dimensions in cm).

44
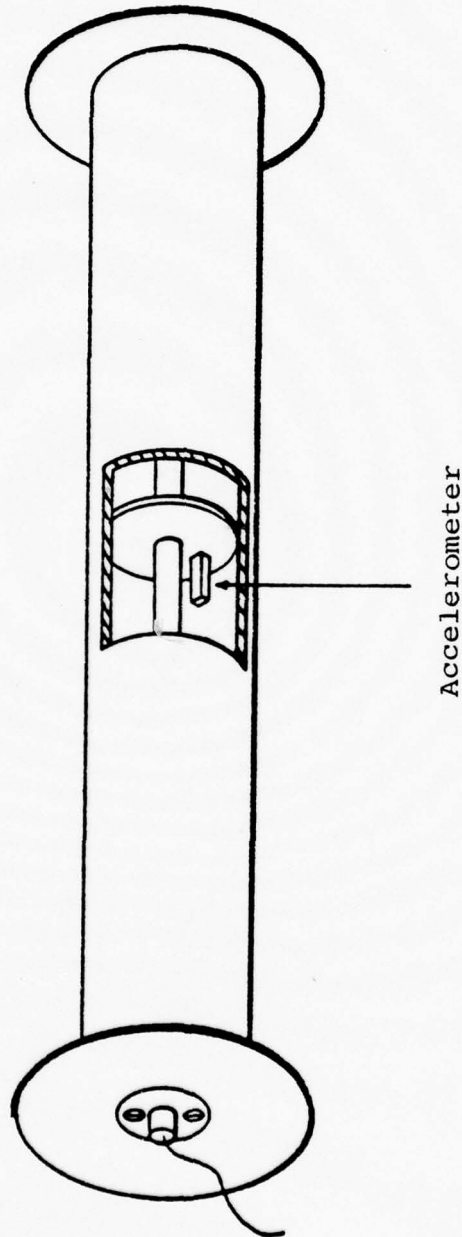
Accelerometer

Fig. 6 A cutaway sketch of a cylinder with accelerometer.
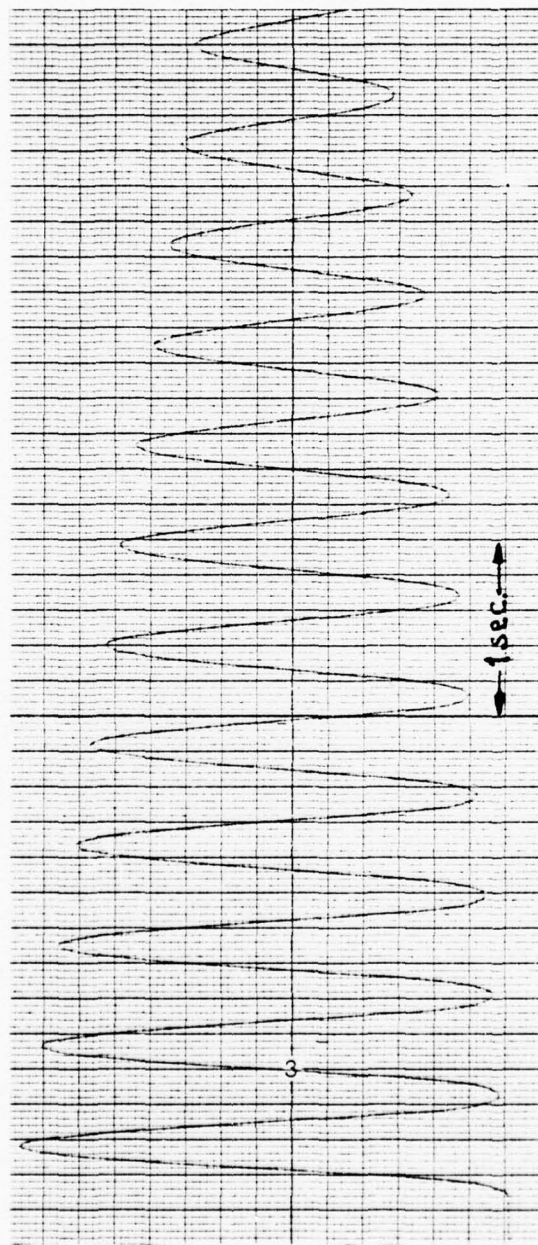
Fig. 7 Displacement trace of a "plucked" cylinder.

46
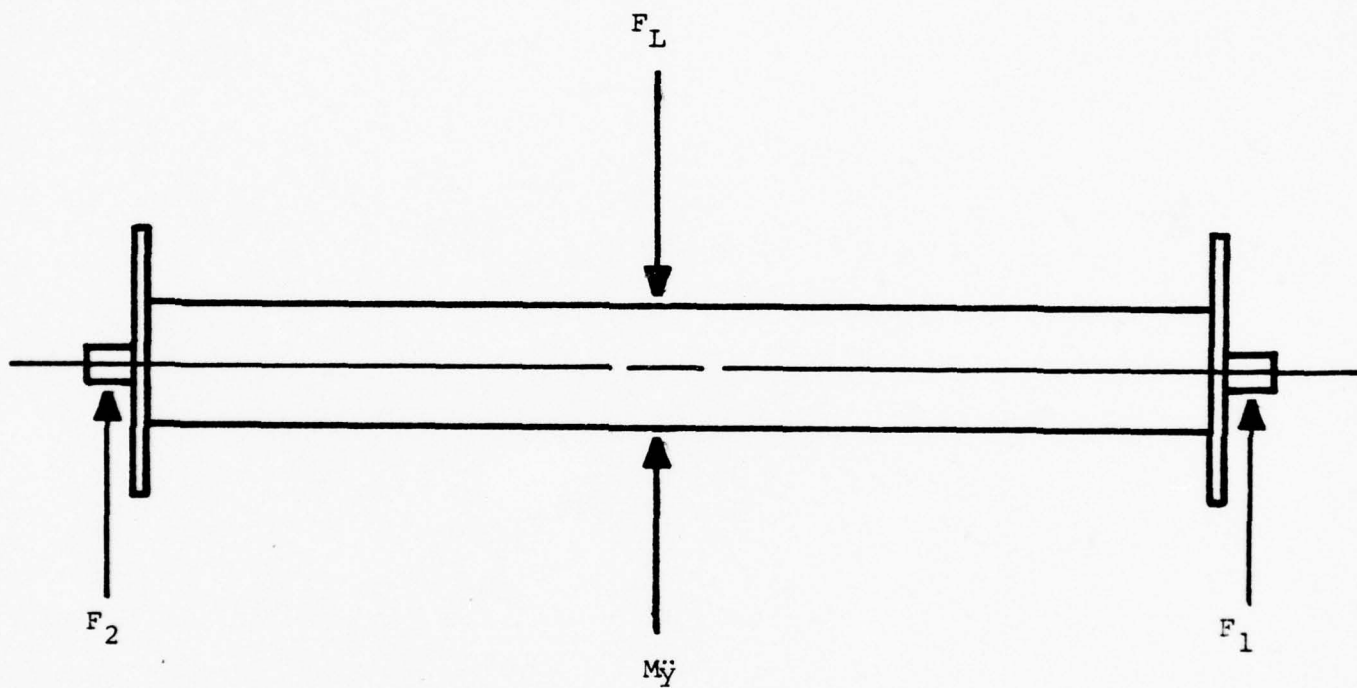
Fig. 8   Freebody diagram of the
         test cylinder.
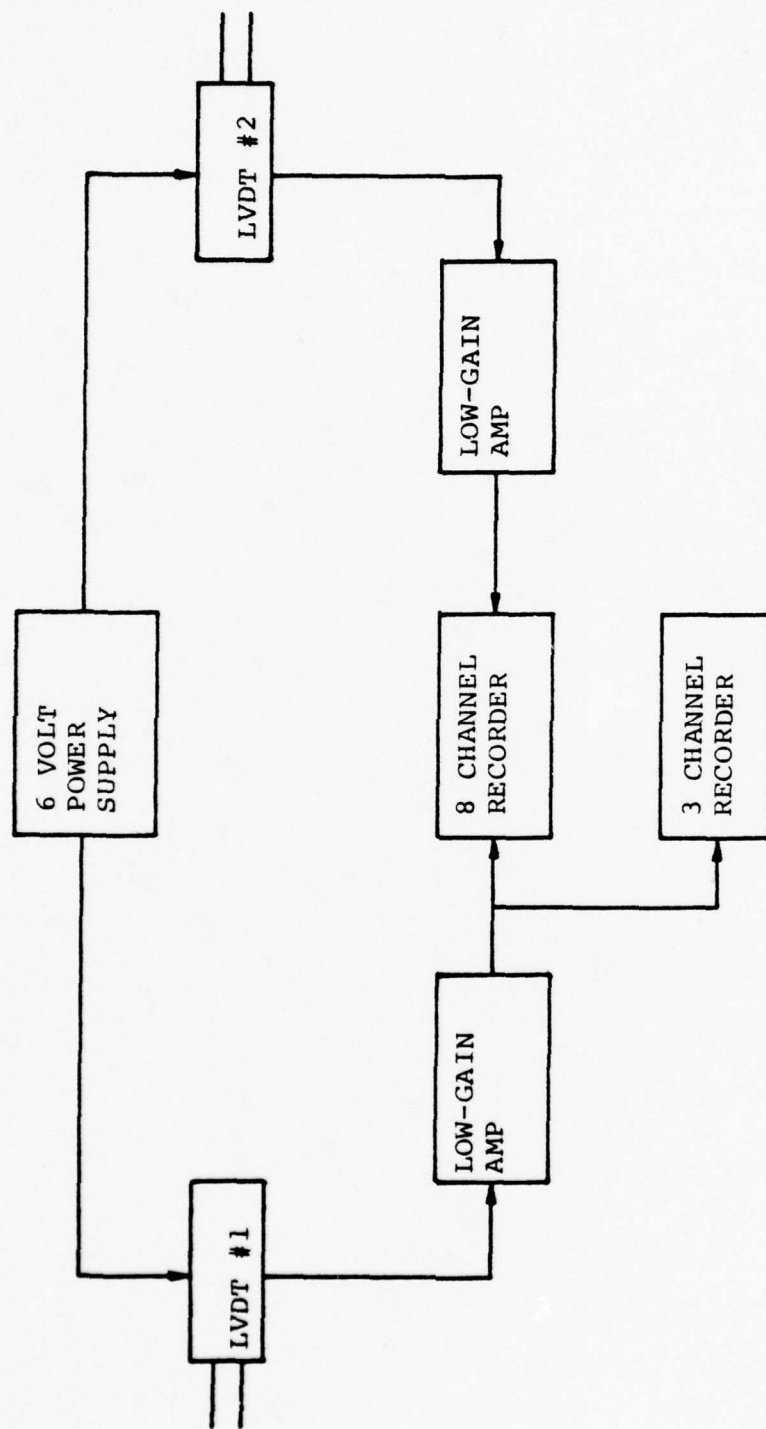
Fig. 9   LVDT (Linear-variable-displacement transducer) electronic circuit.
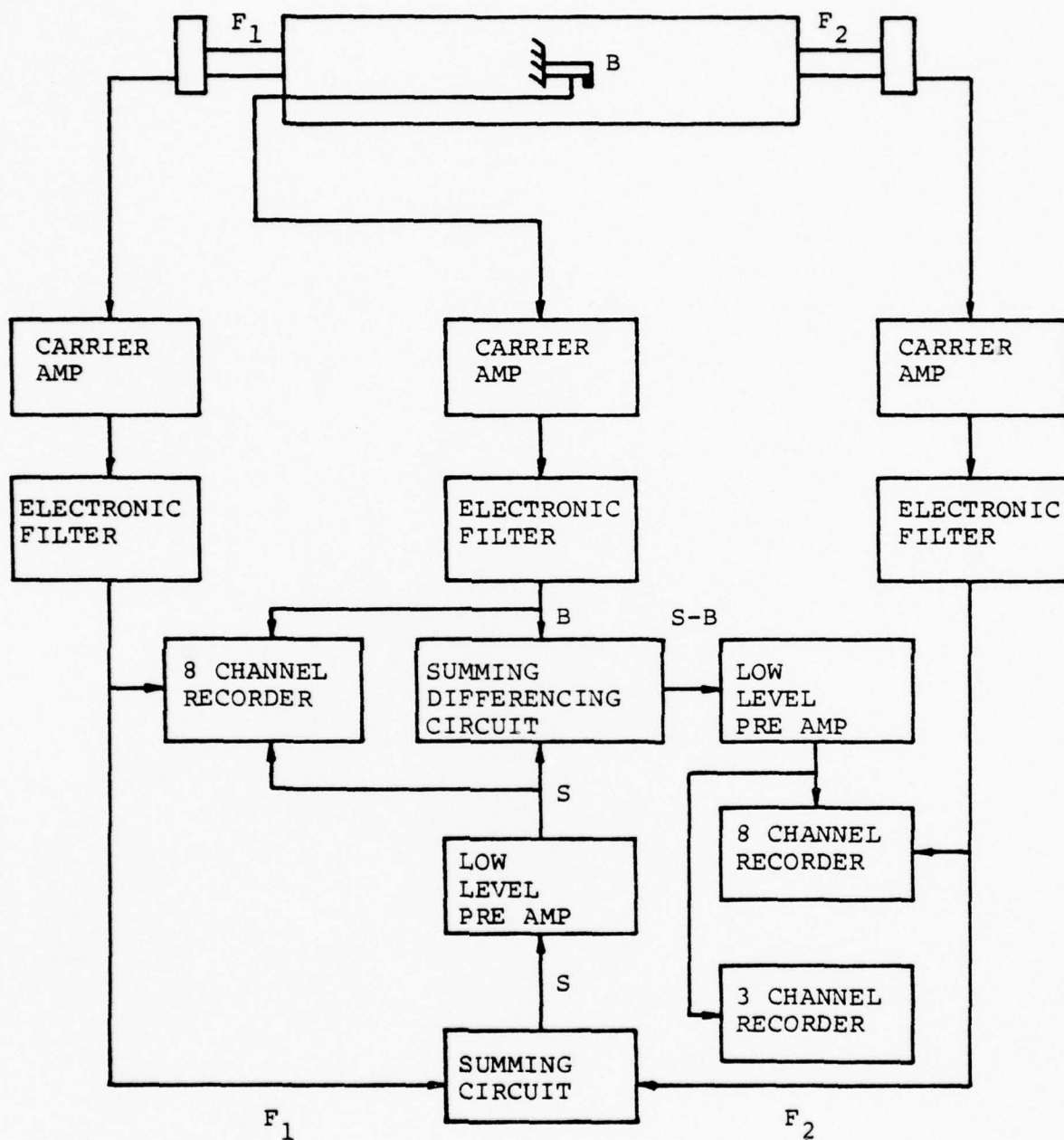
Fig. 10 Force and accelerometer electronic circuits
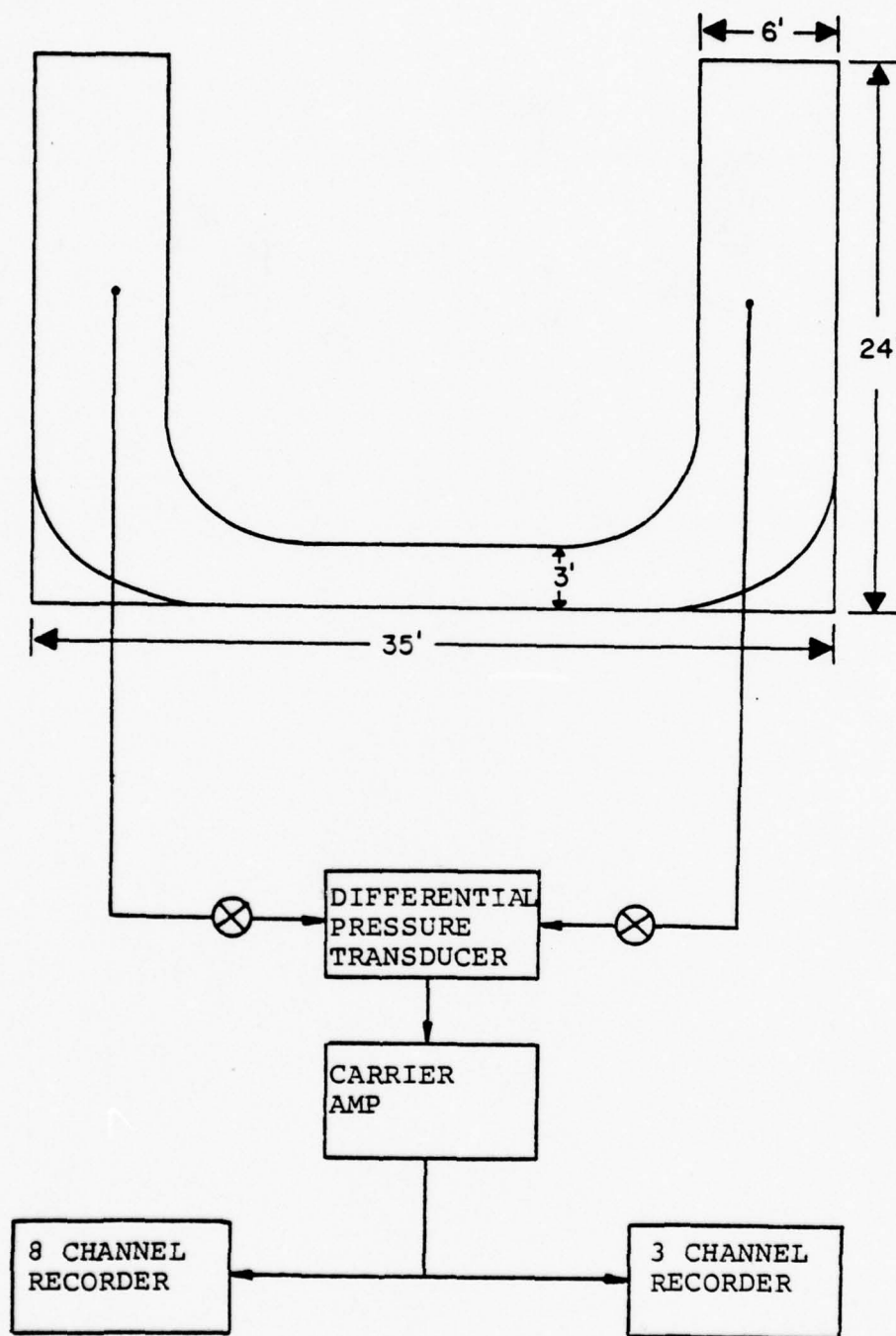
Fig. 11 Differential pressure transducer
and circuitry.
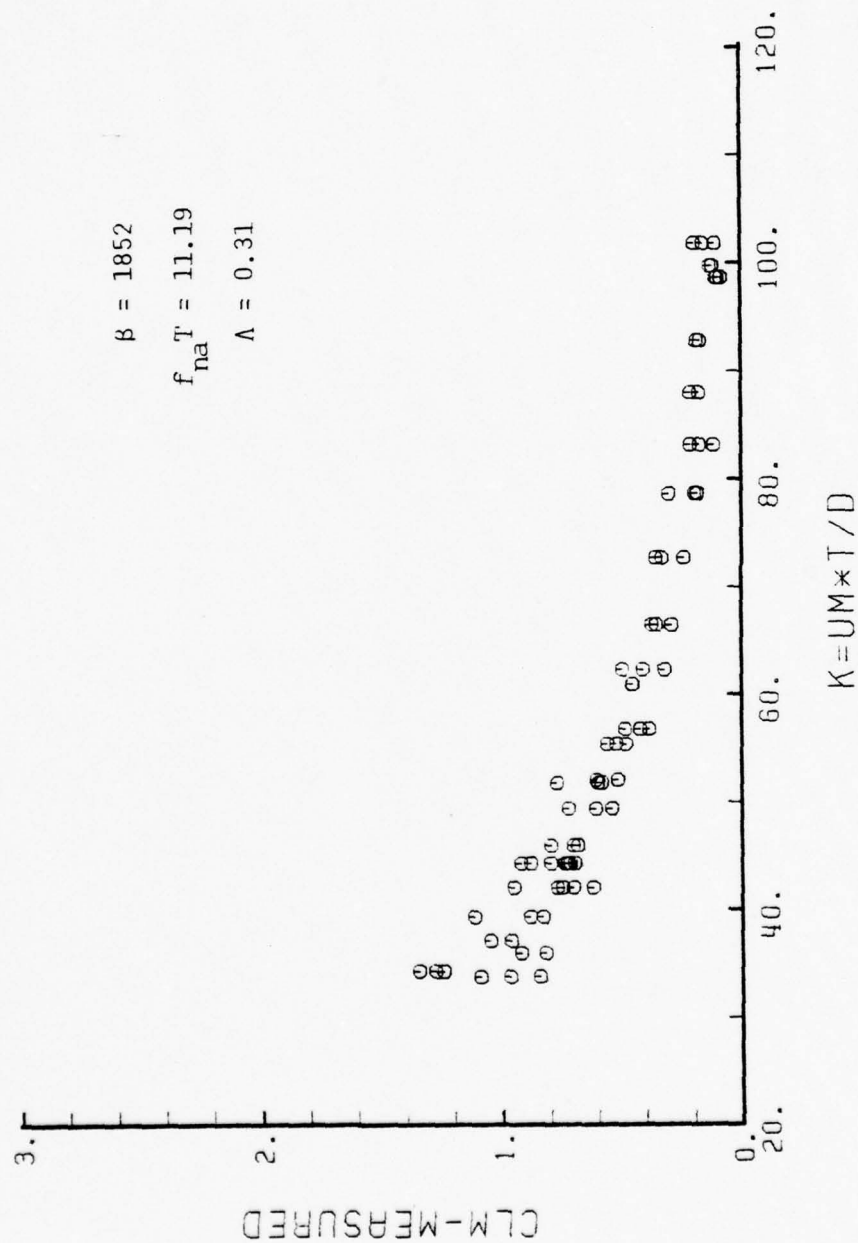
Fig. 12 C_{LM} versus K for a smooth cylinder.

$\beta = 1852$

$f_{na}^{T} = 11.19$

$\Lambda = 0.31$

K=UM*T/D

CLM-MEASURED

$\beta = 1852$

$f_{na}T = 11.18$

$\Lambda = 0.41$

K=UM*T/D

CLM-MEASURED

Fig. 13 C_{LM} versus K for a rough cylinder with $\zeta_\omega = 0.060$

β = 1852

$f_{na}T$ = 10.59

Λ = 0.19

CLM-MEASURED

K=UM*T/D
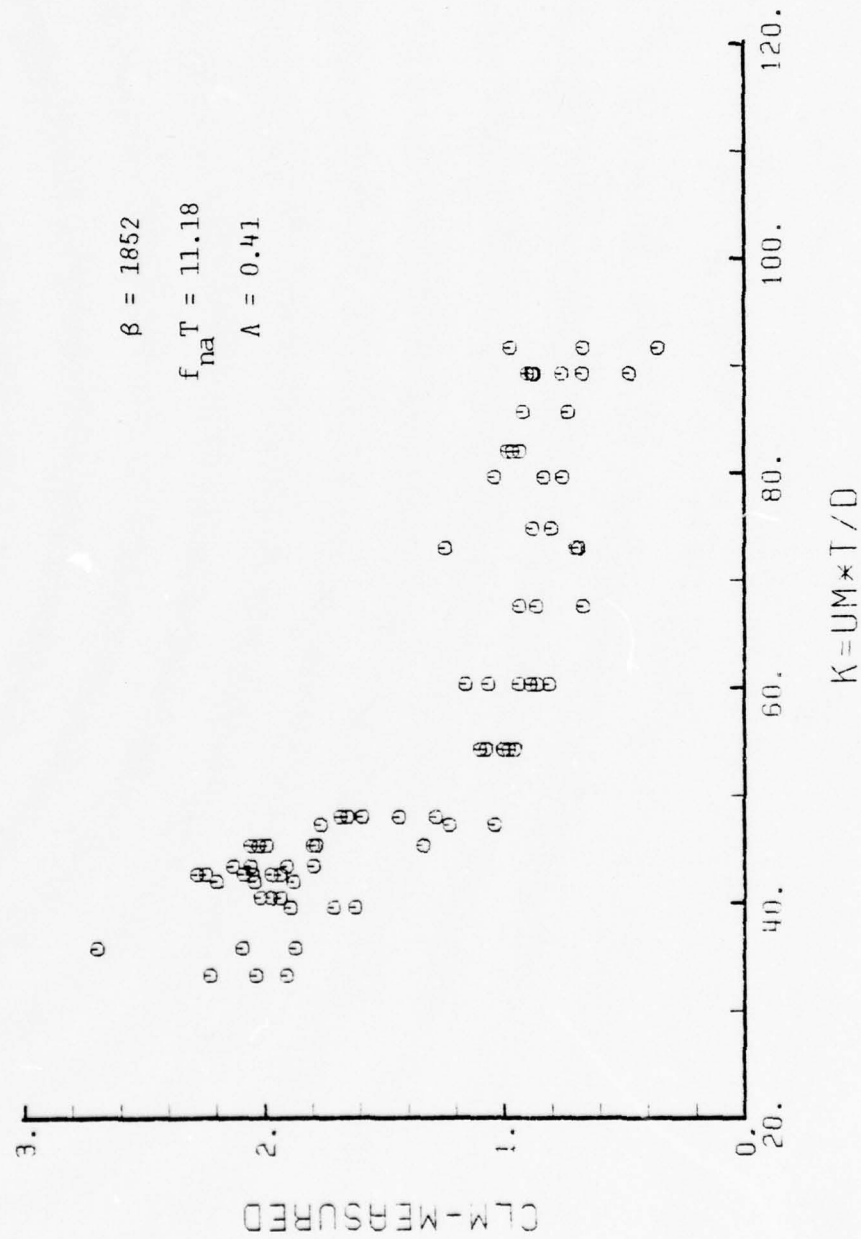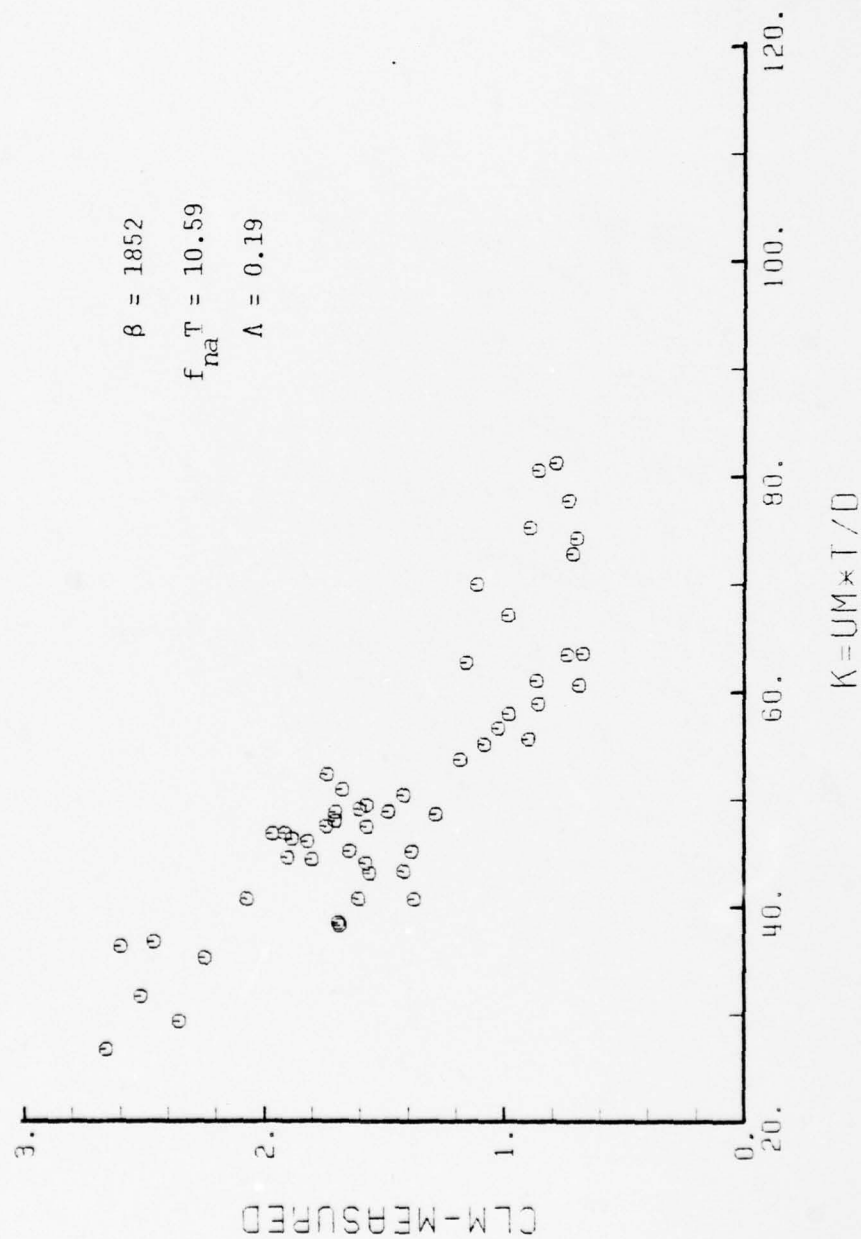
Fig. 14 C_{LM} versus K for a rough cylinder with ζ_ω=0.03
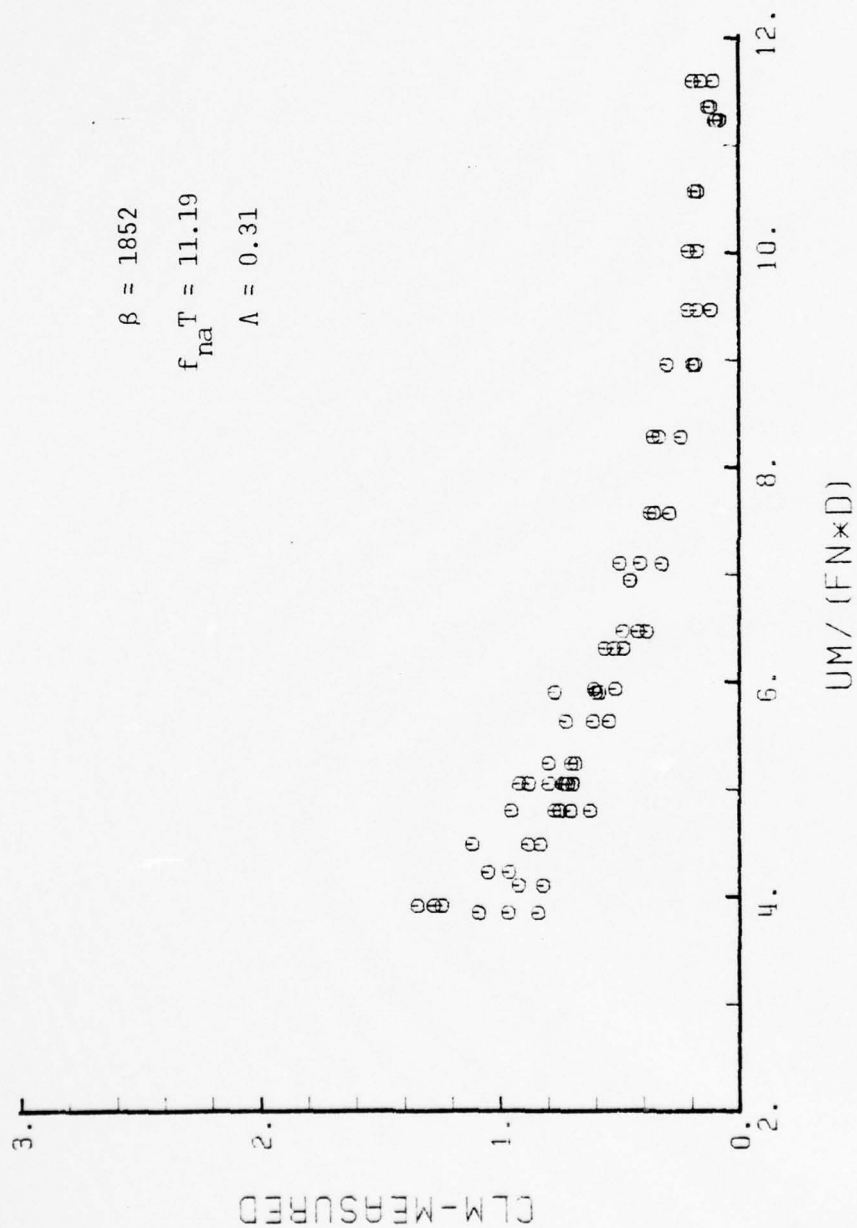
Fig. 15 C_{LM} versus U_r for a smooth cylinder.

$\beta = 1852$

$f_{na}T = 11.19$

$\Lambda = 0.31$

UM/ (FN*D)

CLM-MEASURED

54

$\beta = 1852$

$f_{na}T = 11.18$

$\Lambda = 0.41$

UM/(FN*D)

CLM-MEASURED
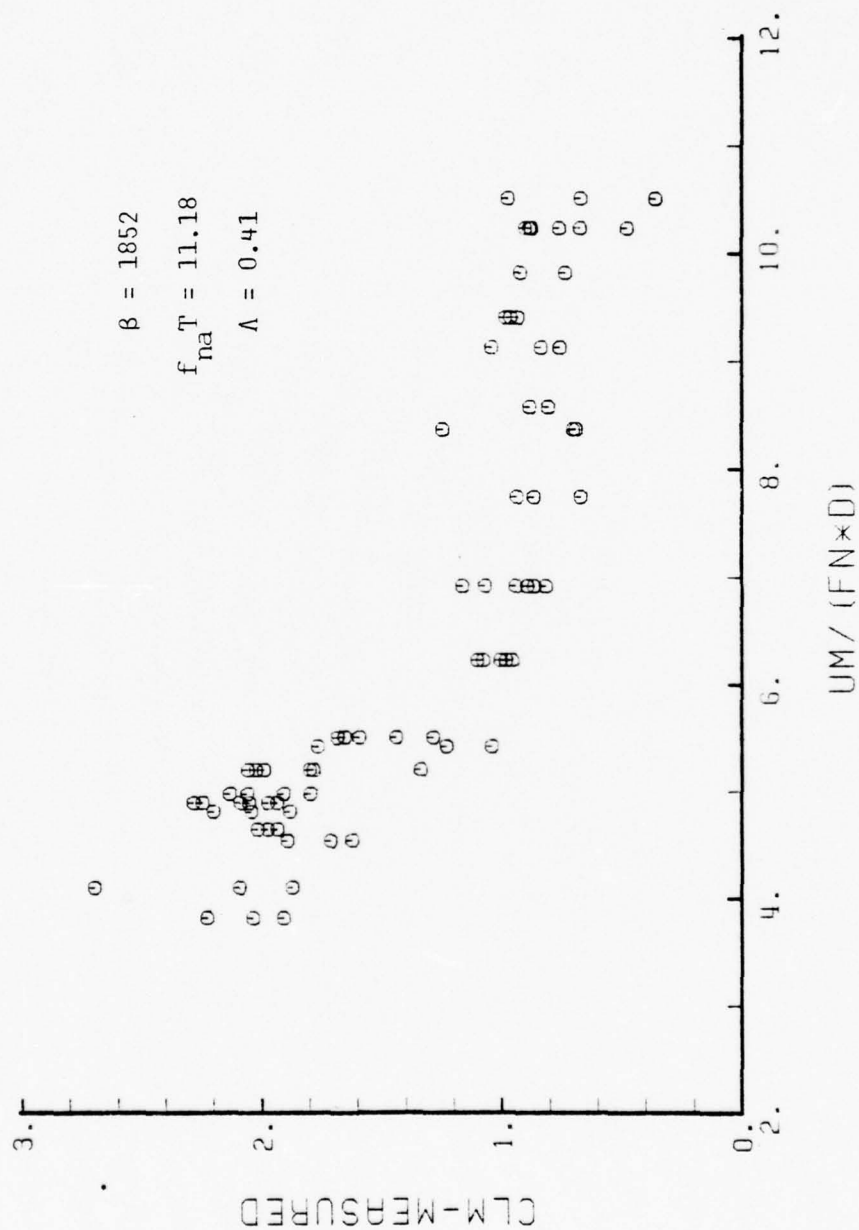
Fig. 16 C_{LM} versus U_r for a rough cylinder with $\zeta_\omega = 0.060$
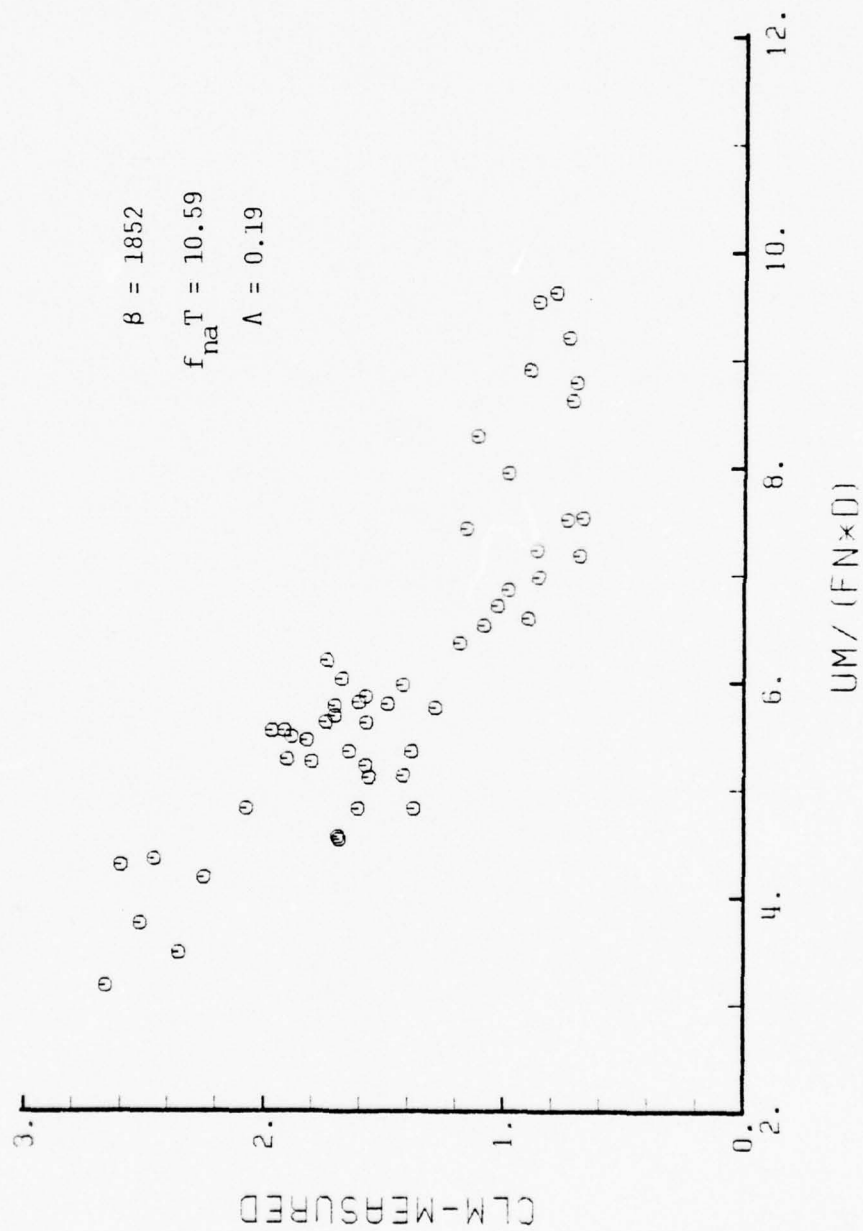
Fig. 17 C_{LM} versus U_r for a rough cylinder with $\zeta_\omega = 0.03$

Fig. 18 C_{LM} versus $\frac{f_v}{f_c}$ for a smooth cylinder

$\beta = 1852$

$f_{na}T = 11.19$

$\Lambda = 0.31$

FV/FC

CLM-MEASURED
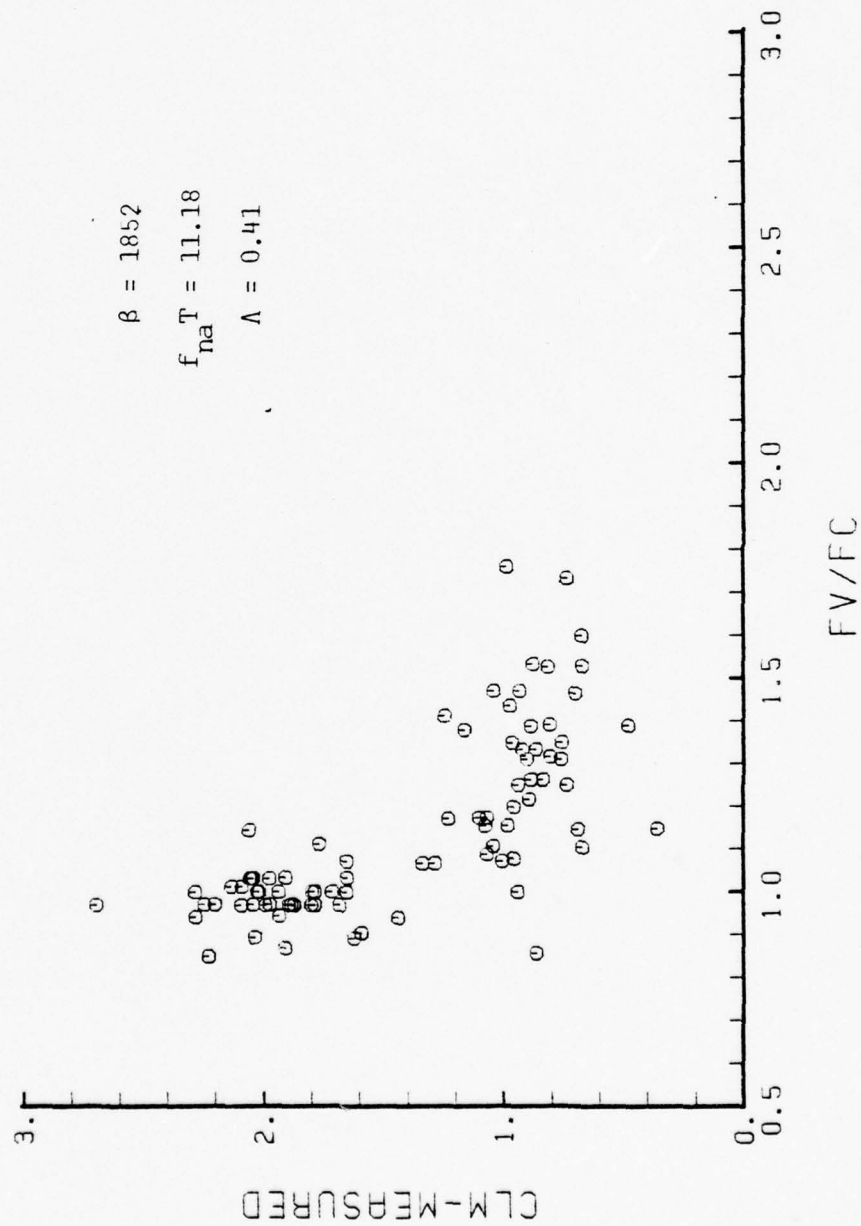
Fig. 19 C_{LM} versus f_V/f_C for a rough cylinder with $\zeta_\omega = 0.060$

$\beta = 1852$

$f_{na}T = 11.18$

$\Lambda = 0.41$

FV/FC

CLM-MEASURED
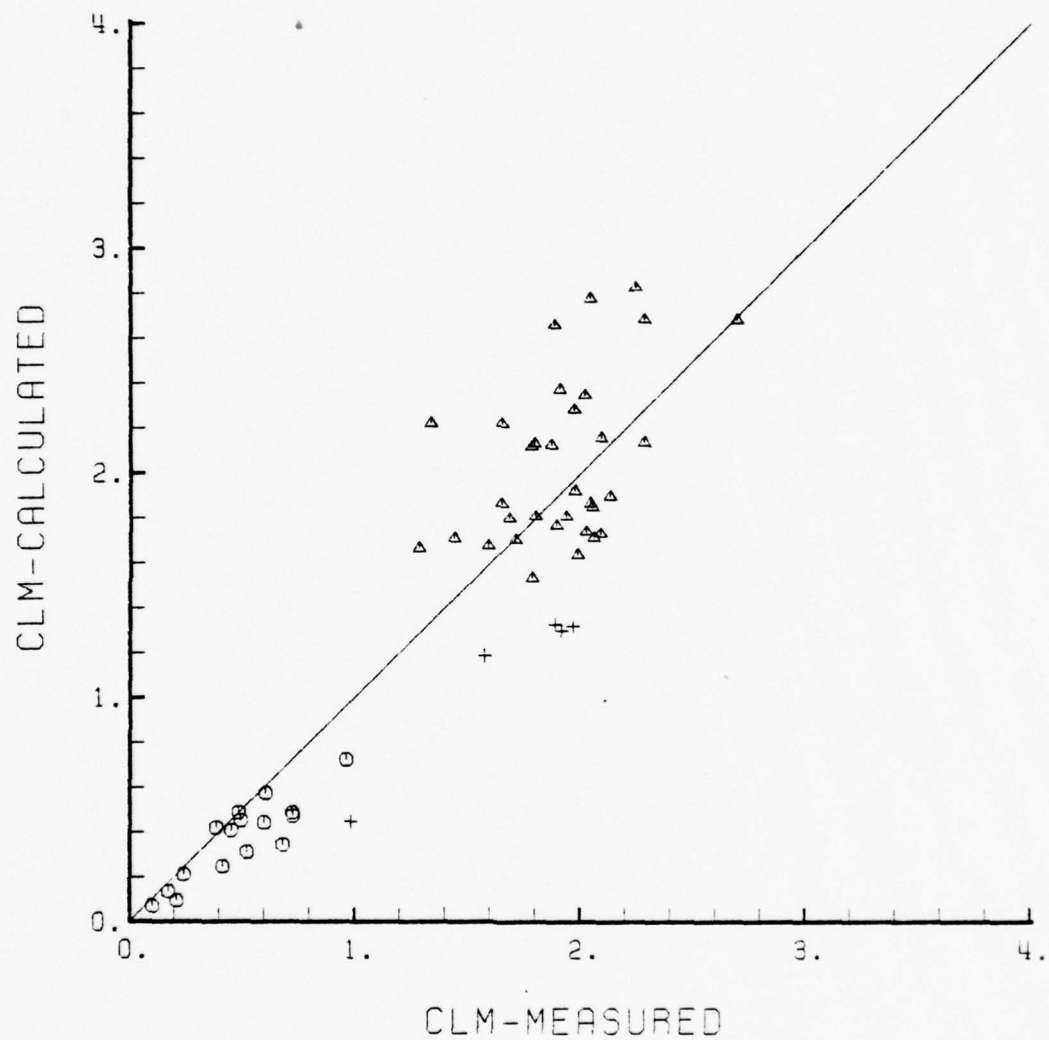
Fig. 20 C_{LM}^C versus C_{LM} for smooth and rough cylinders in the synchronization region
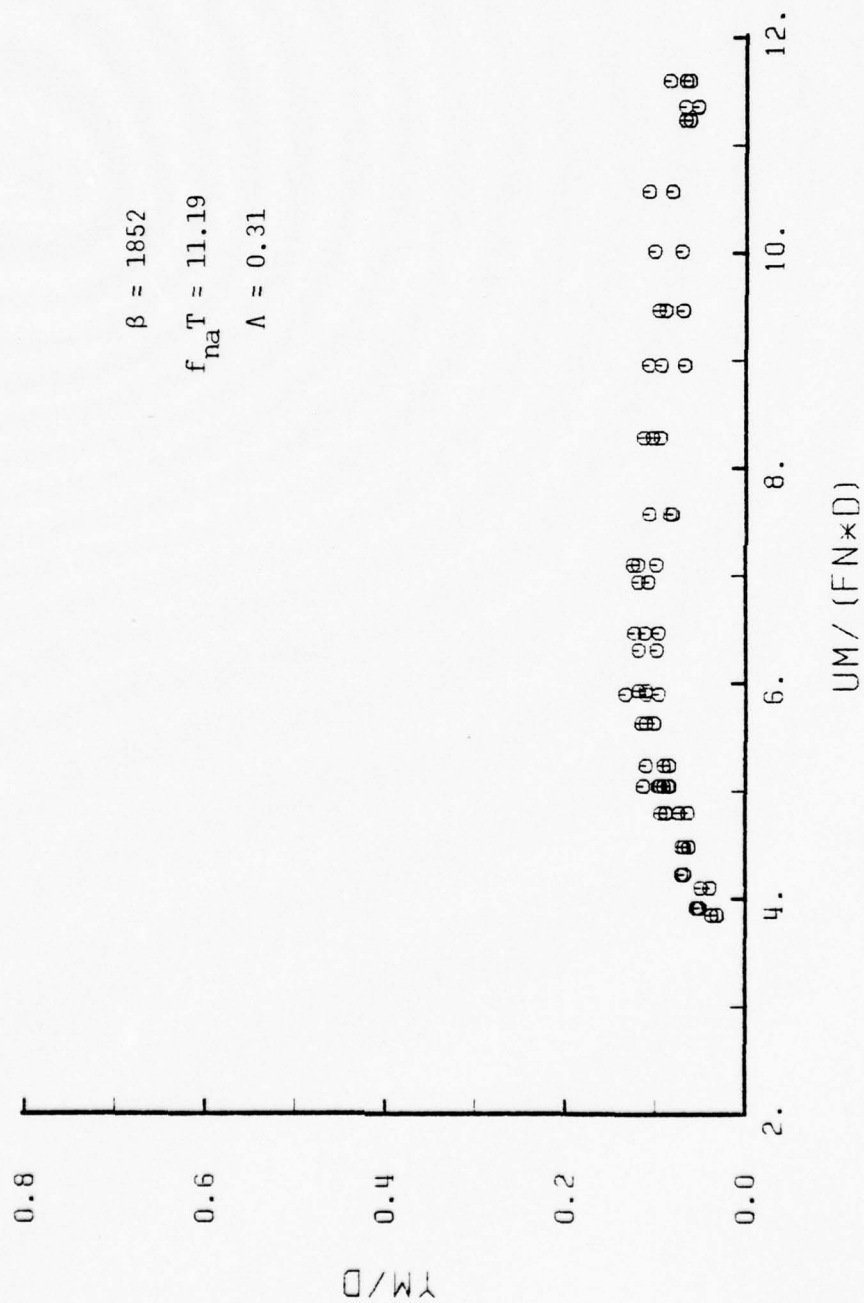
Fig. 21 Y_M/D versus U_r for a smooth cylinder

$\beta = 1852$

$f_{na}T = 11.19$

$\Lambda = 0.31$

60
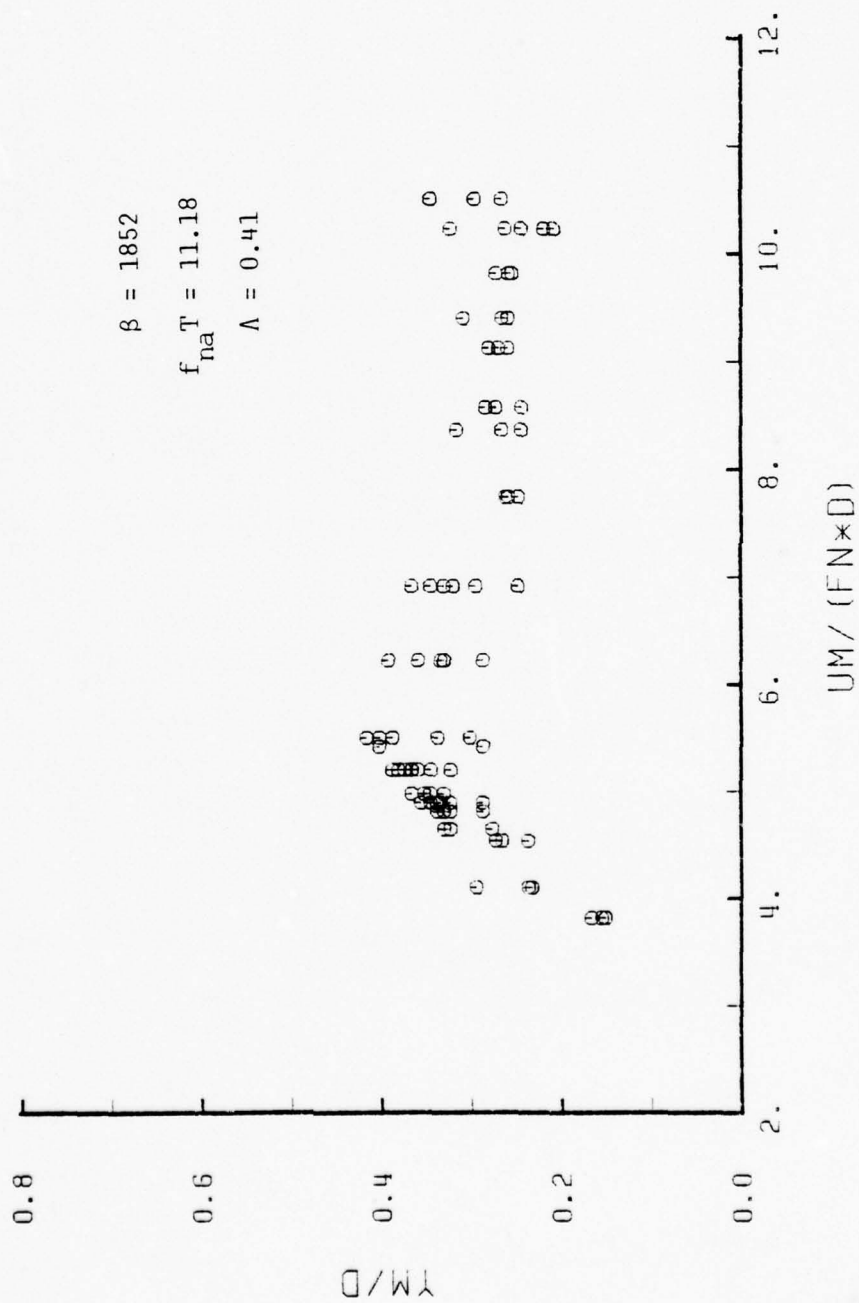
Fig. 22 Y_M/D versus U_r for a rough cylinder with $\zeta_\omega = 0.060$

$\beta = 1852$

$f_{na}T = 11.18$

$\Lambda = 0.41$

61
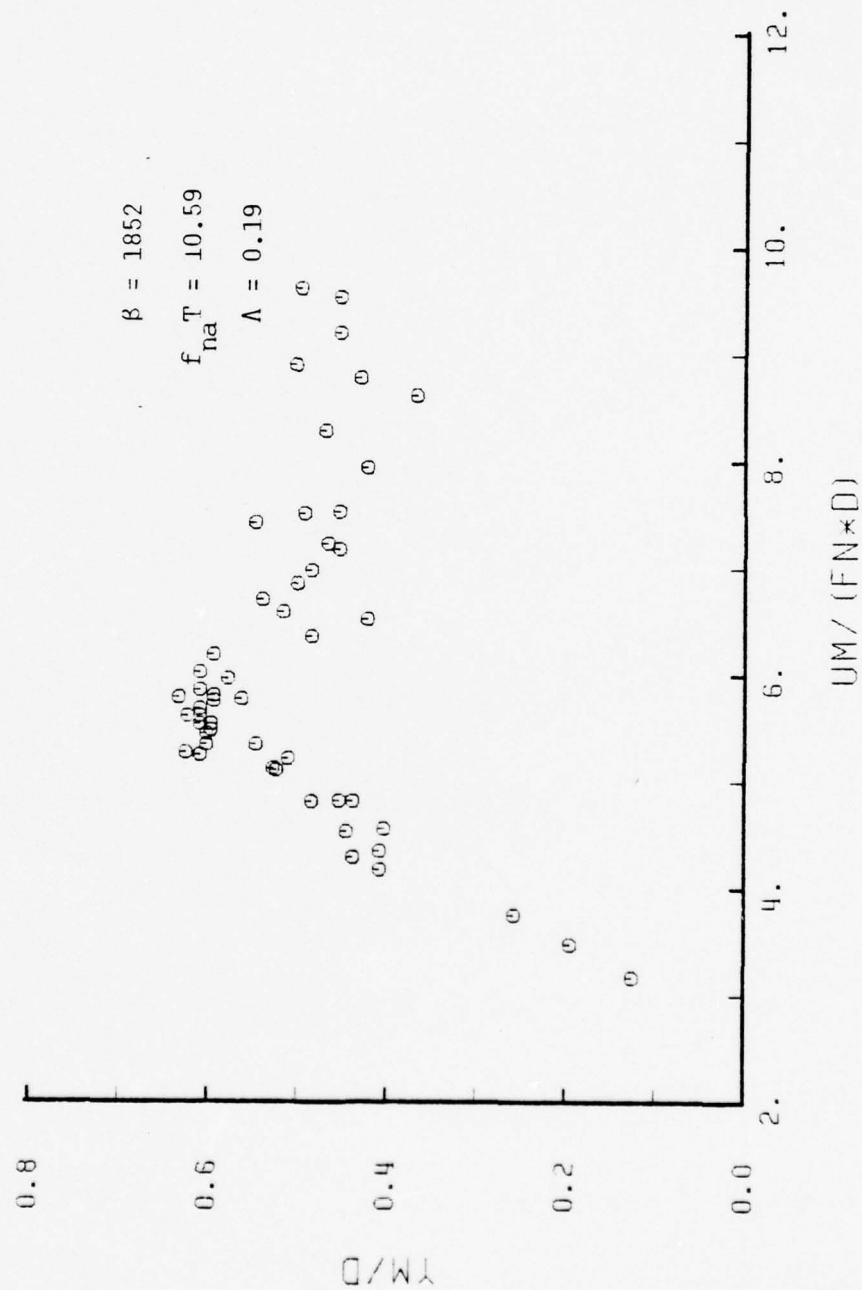
Fig. 23 Y_M/D versus U_r for a rough cylinder with $\zeta_\omega = 0.030$

$\beta = 1852$

$f_{na}T = 11.19$

$\Lambda = 0.31$

$K = UM \ast T / D$

Fig. 24 Y_M/D versus K for a smooth cylinder

Y_M/D
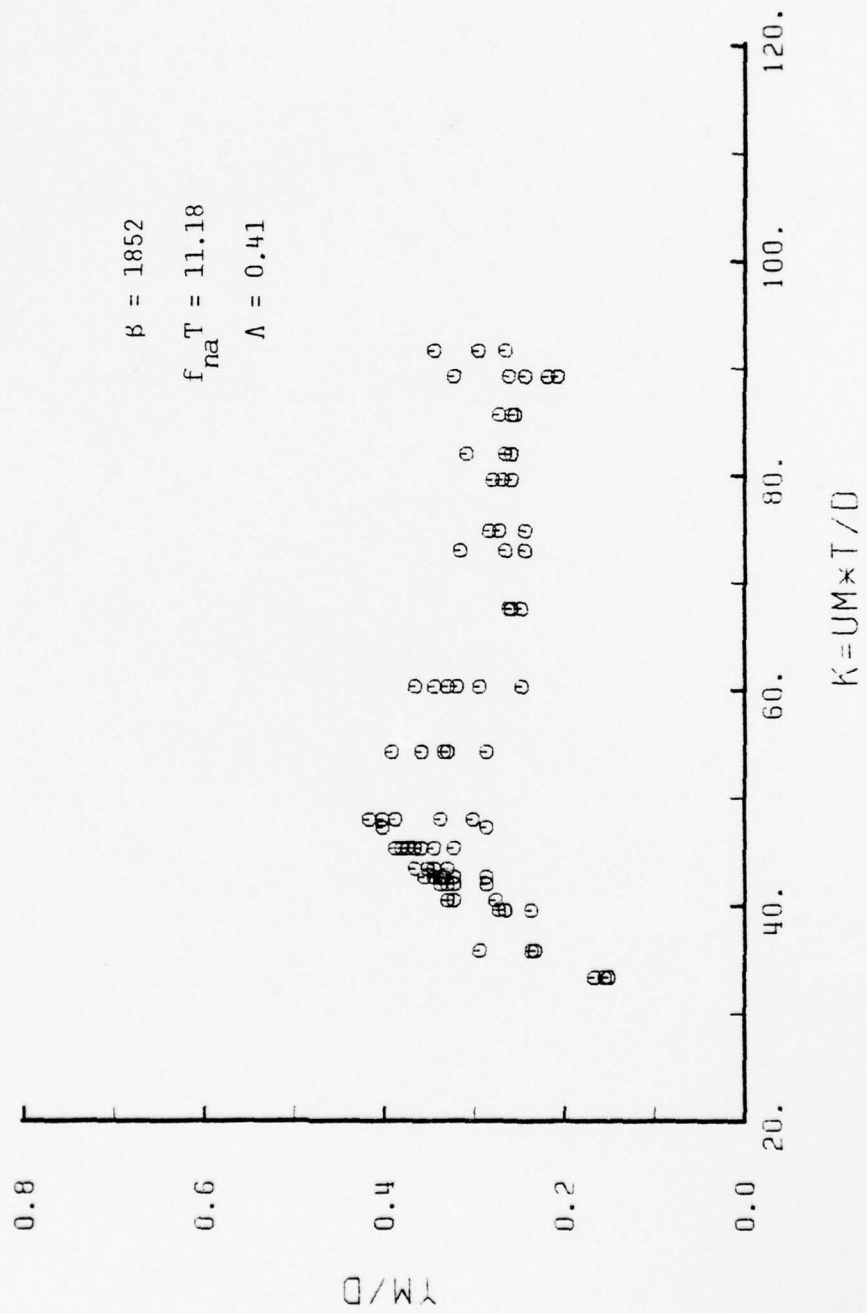
Fig. 25 Y_M/D versus K for a rough cylinder with $\zeta_\omega = 0.060$

β = 1852

$f_{na}T$ = 10.59

Λ = 0.19

K=UM*T/D

YM/D

Fig. 26 Y_M/D versus K for a rough cylinder with ζ_ω =0.03

β = 1852

$f_{na}T$ = 11.19

Λ = 0.31

250000.0

200000.0

150000.0

100000.0

50000.0

0.0

RE

0.8

0.6

0.4

0.2

0.0

YM/D
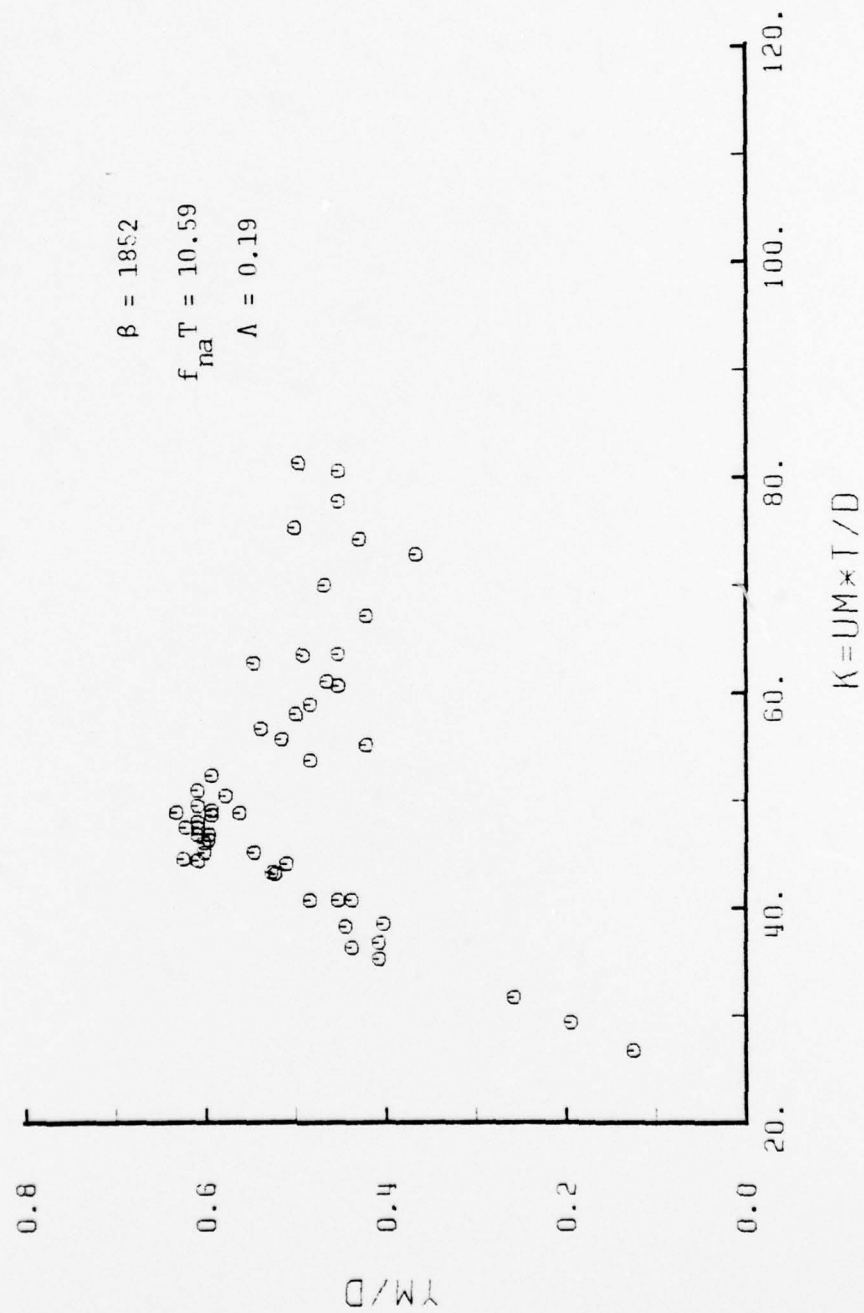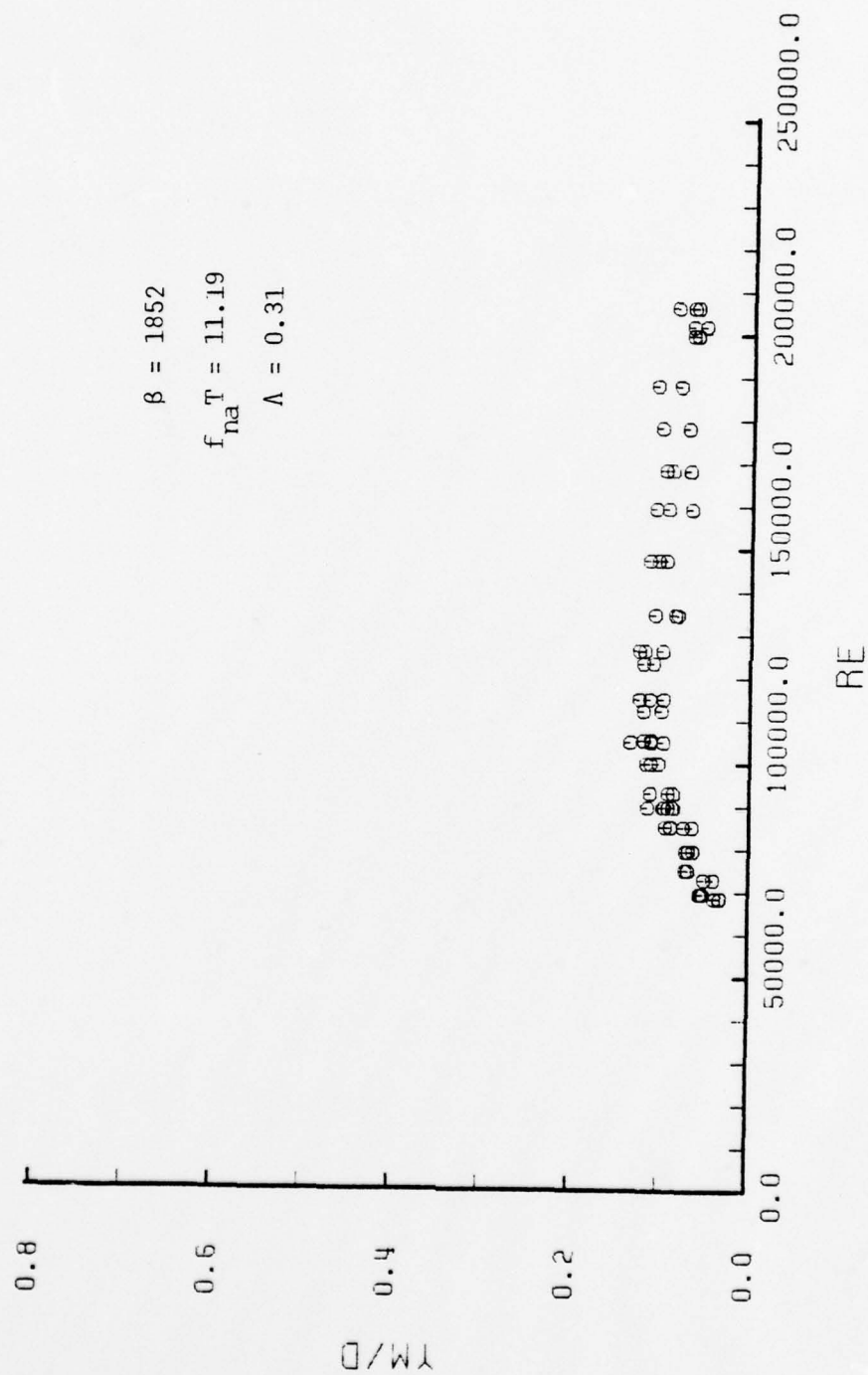
Fig. 27 Y_M/D versus Re for a smooth cylinder
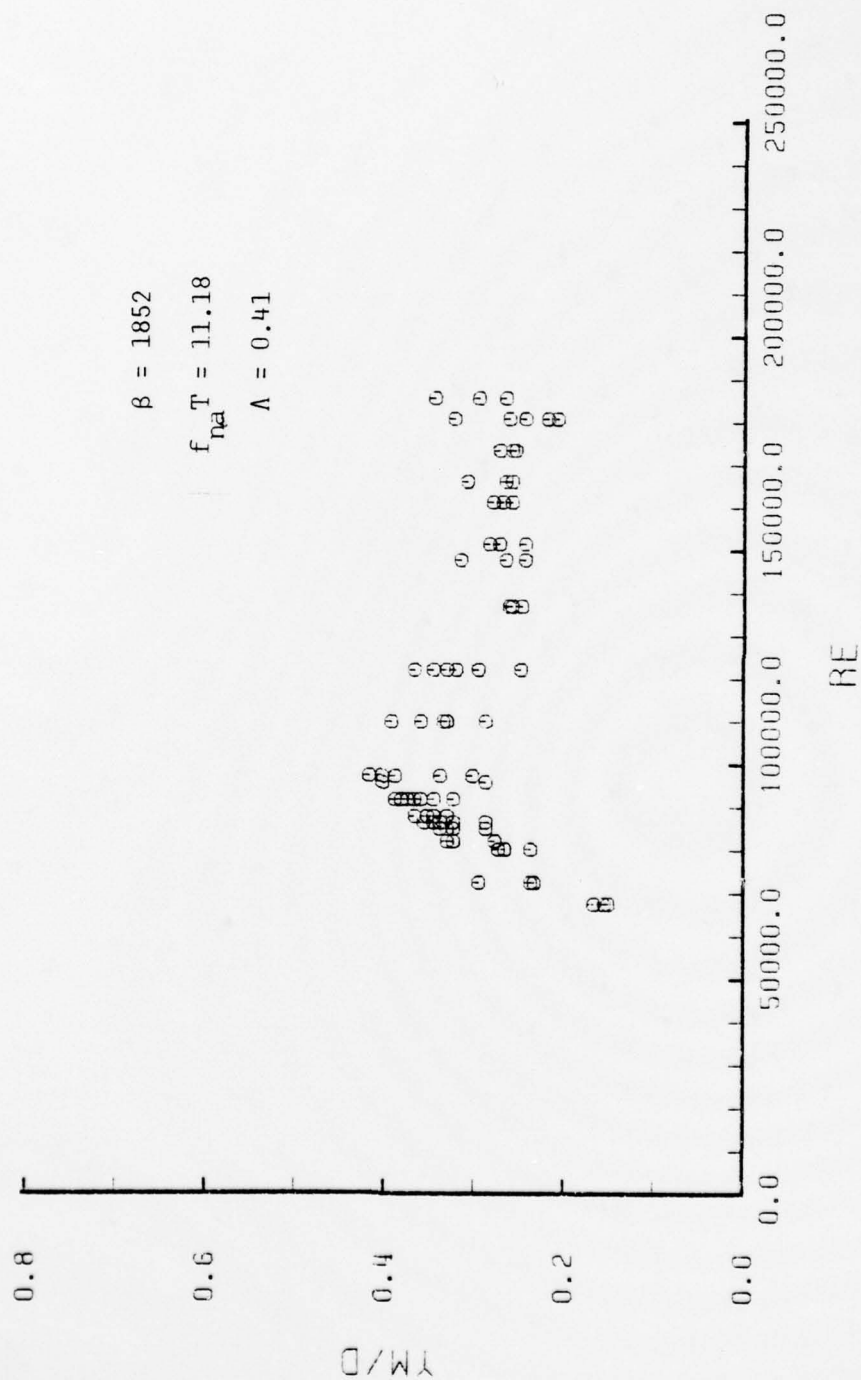
Fig. 28 Y_M/D versus Re for a rough cylinder with $\zeta_\omega = 0.060$

$\beta = 1852$

$f_{na}T = 11.18$

$\Lambda = 0.41$

RE

YM/D
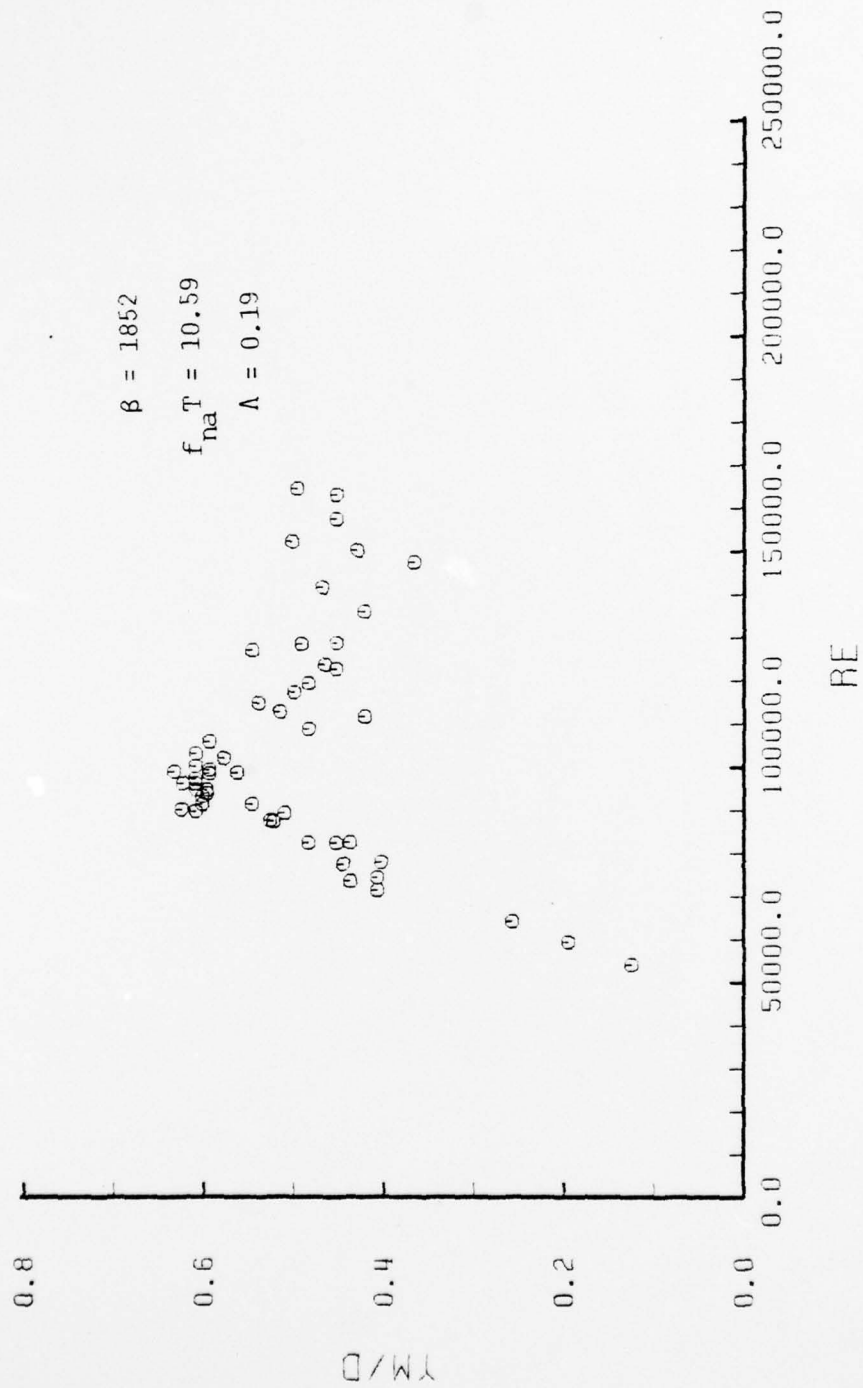
Fig. 29 Y_M/D versus Re for a rough cylinder with $\zeta_w = 0.03$
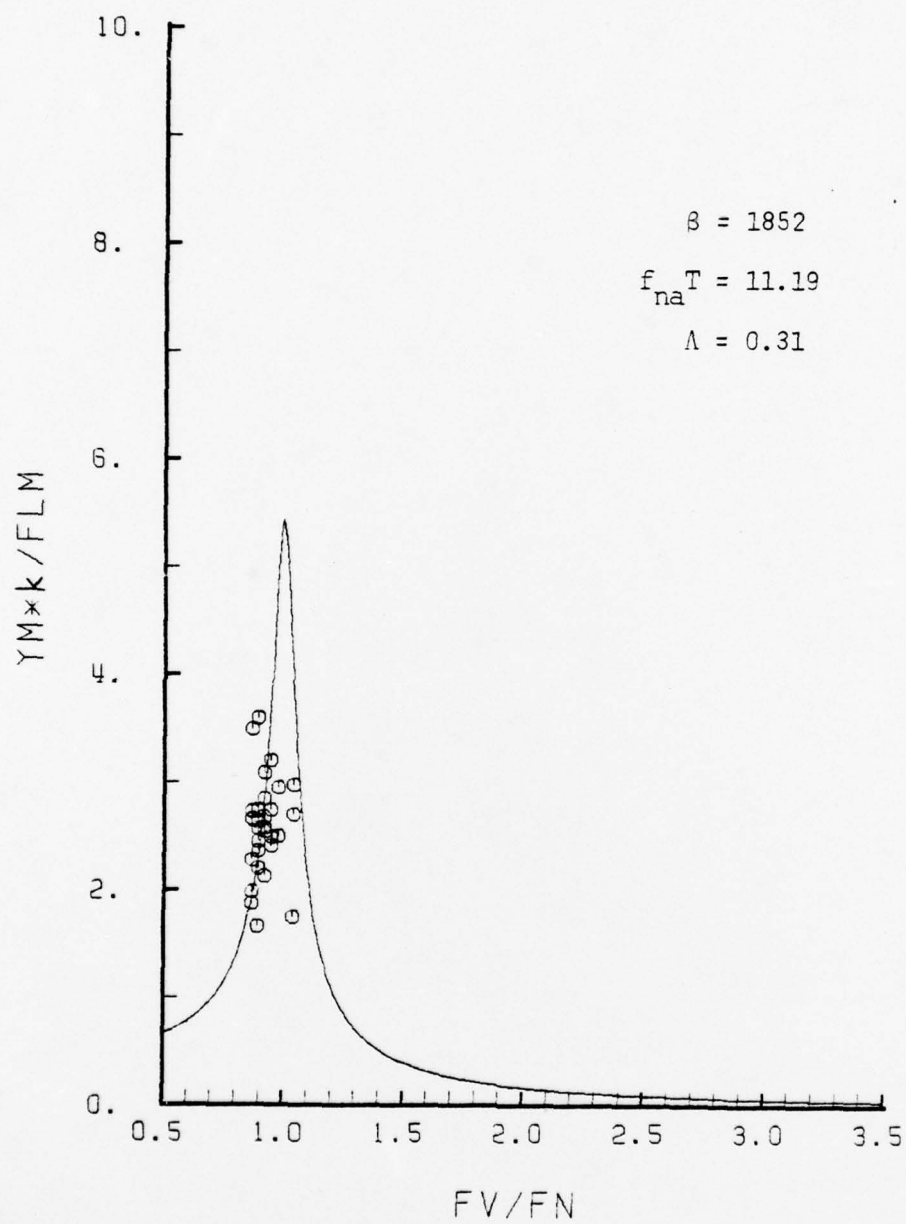
$\beta = 1852$

$f_{na}T = 10.59$

$\Lambda = 0.19$

Fig. 30 $Y_M k/F_{LM}$ versus f_v/f_n for a smooth
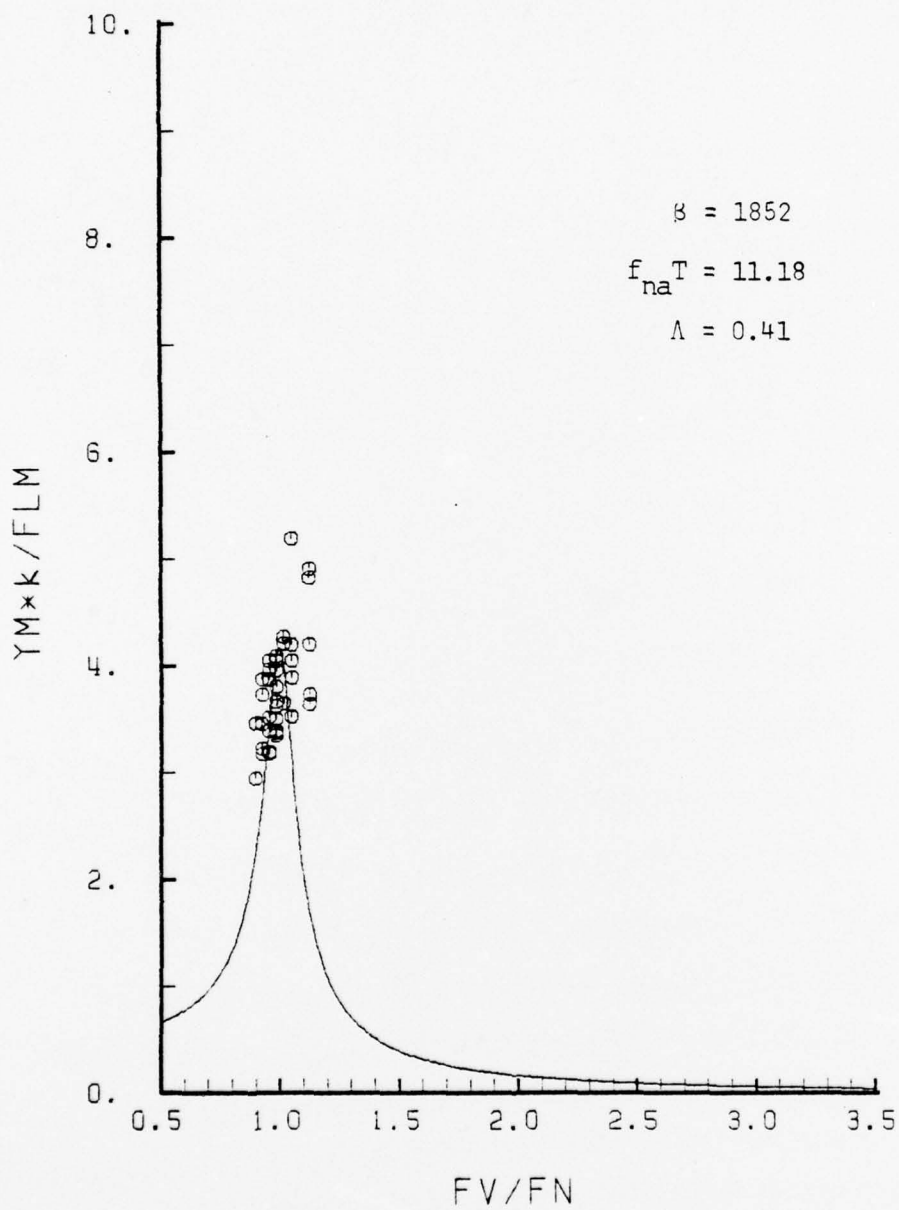cylinder in the synchronization region

Fig. 31 $Y_M k/F_{LM}$ versus f_v/f_n for a rough cylinder
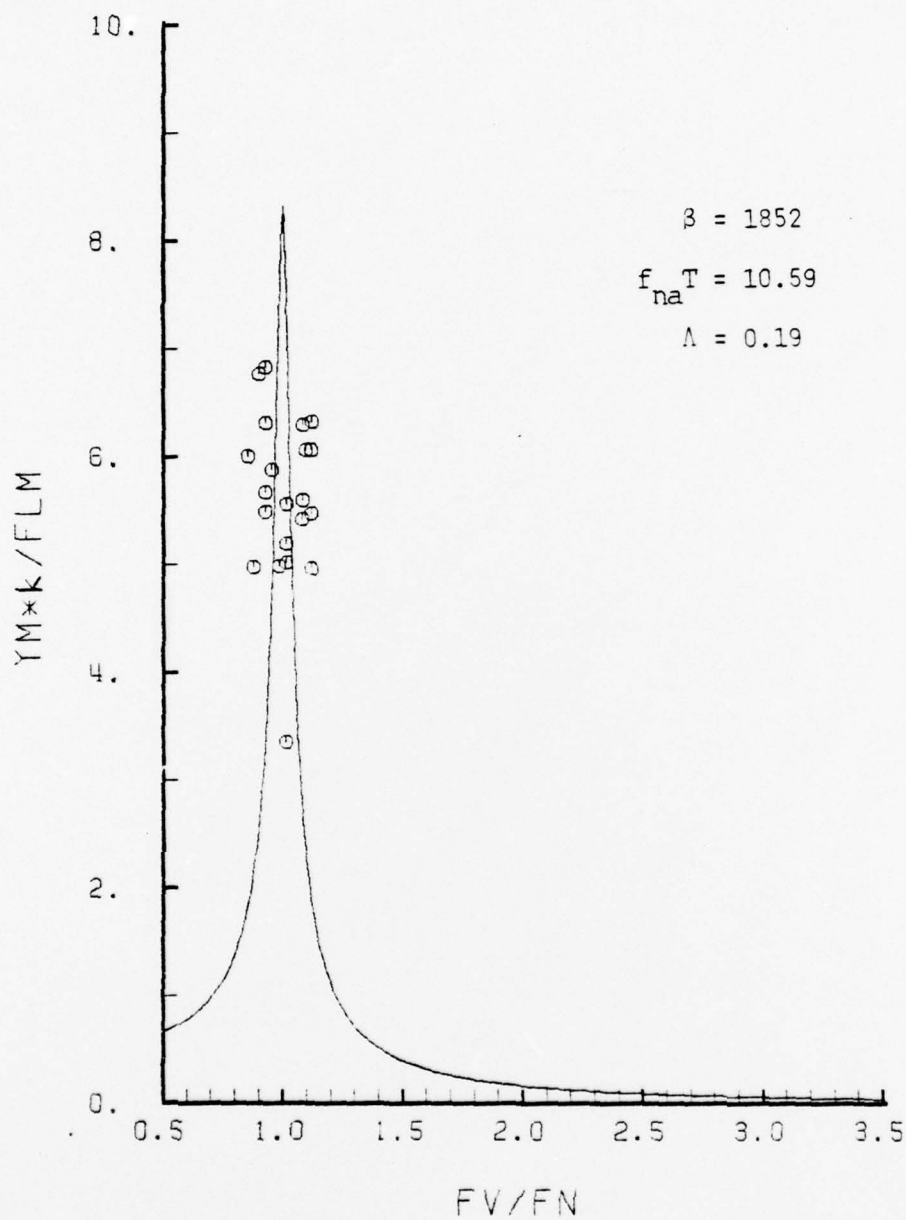with $\zeta_\omega = 0.060$ in the synchronization region

70

Fig. 32 $Y_M k/F_{LM}$ versus f_v/f_n for a rough cylinder with $\zeta_\omega = 0.03$ in the synchronization region

71
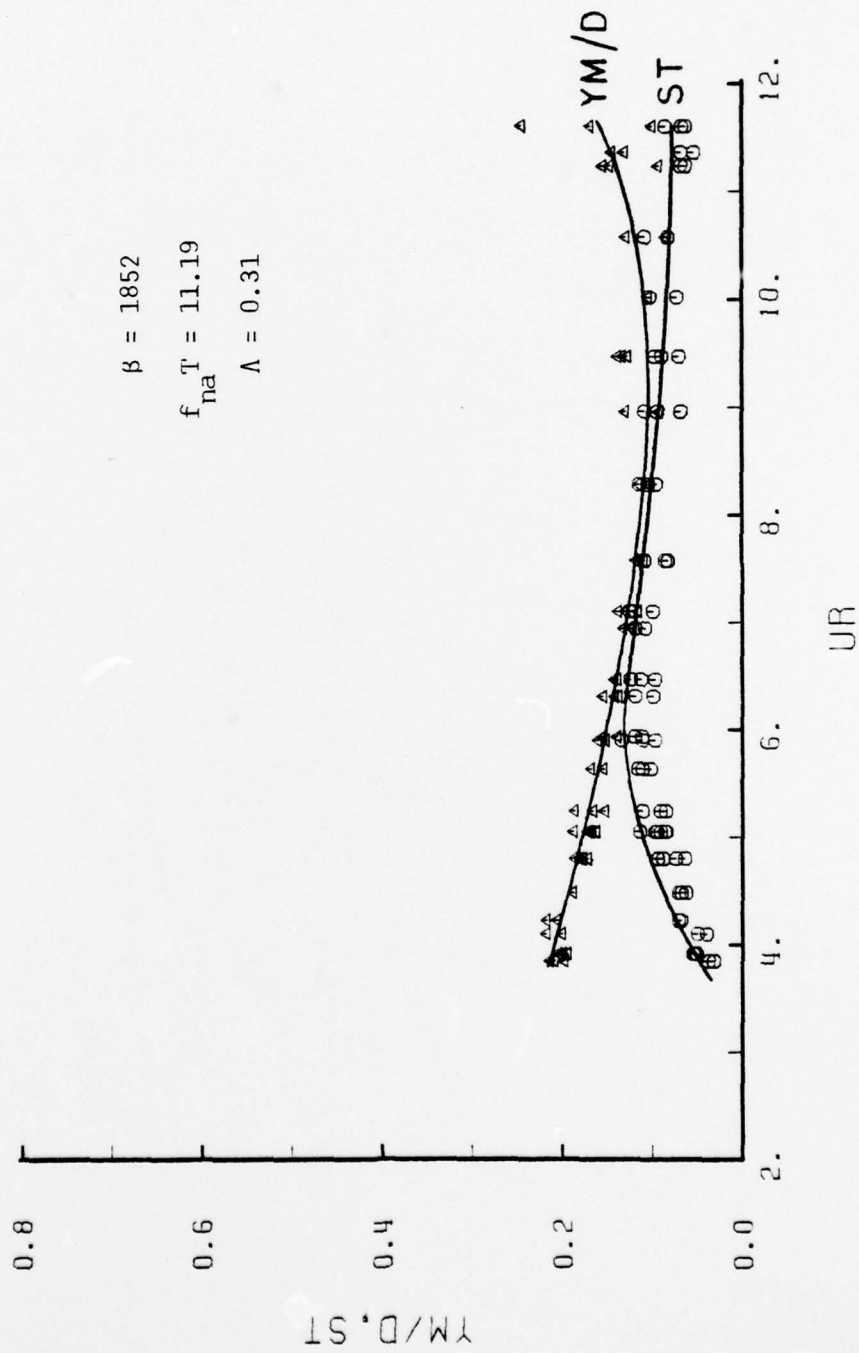
Fig. 33 Y_M/D and St versus U_r for a smooth cylinder

$\beta = 1852$

$f_{na}^T = 11.19$

$\Lambda = 0.31$
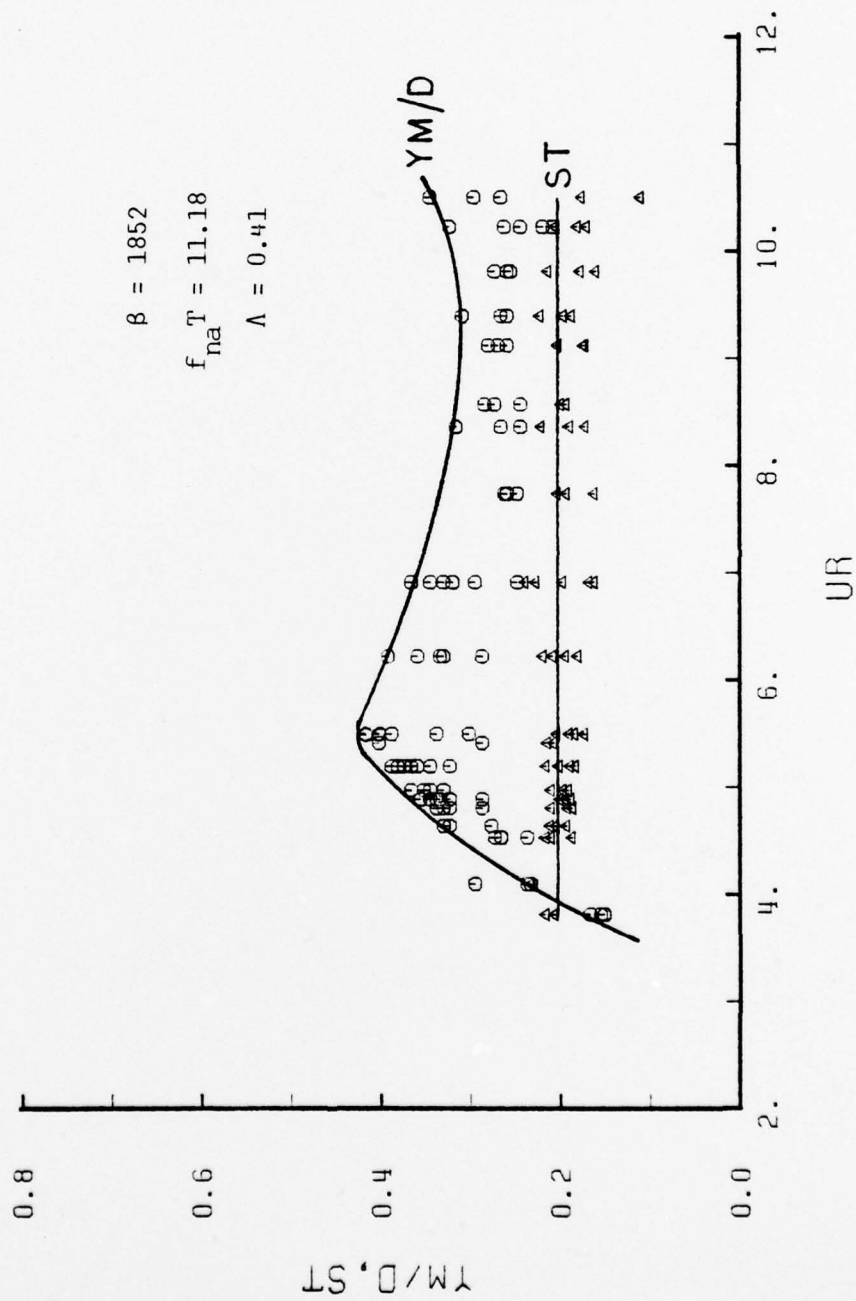
YM/D

ST

UR

YM/D, ST

Fig. 34 Y_M/D and St versus U_r for a rough cylinder with $\zeta_\omega = 0.060$
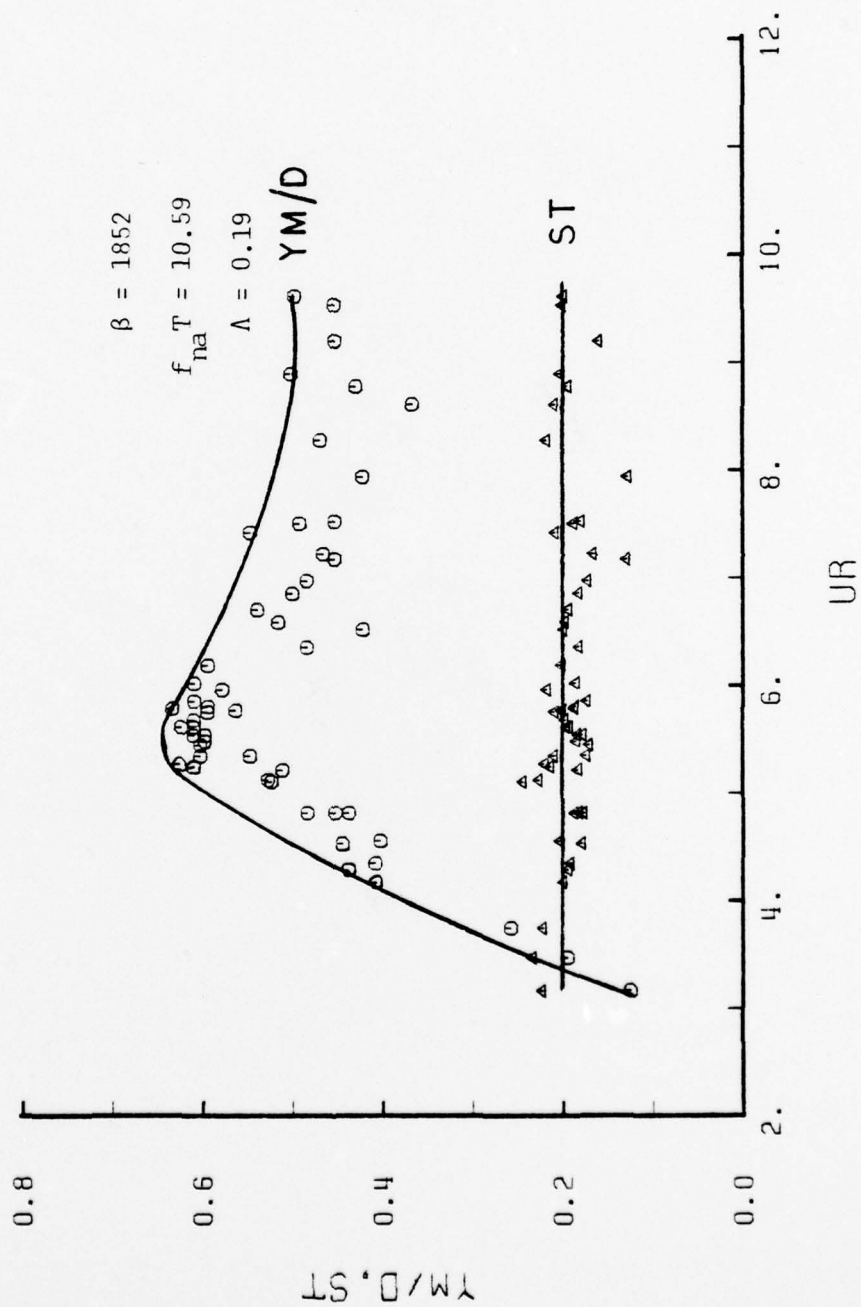
Fig. 35 Y_M/D and St versus U_r for a rough cylinder with $\zeta_\omega = 0.03$

$\beta = 1852$

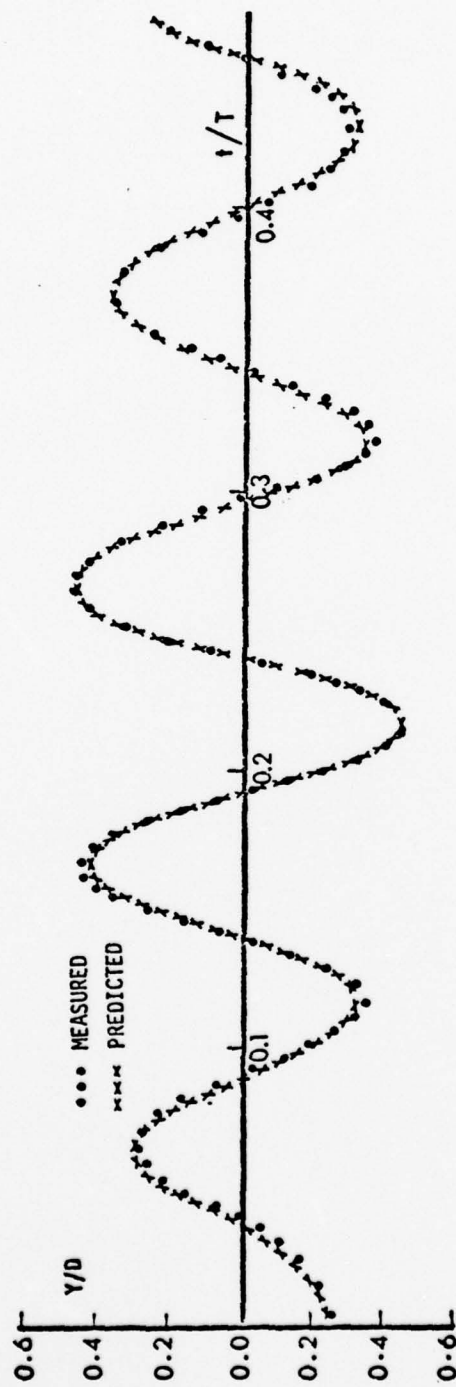$f_{na}T = 10.59$

$\Lambda = 0.19$

74

Fig. 36 Measured and predicted relative displacements as a function of time for $U_r = 5.7$

LIST OF REFERENCES

1. Sarpkaya, T., "Unidirectional Periodic Flow About Bluff Bodies," Technical Report No. NPS-69SL77051, Naval Post-graduate School, Monterey, California, 1977.

2. Sarpkaya, T., "Vortex Shedding and Resistance in Harmonic Flow about Smooth and Rough Cylinders at High Reynolds Numbers," Technical Report No. NPS-59SL76021, Naval Postgraduate School, Monterey, California, 1976.

3. Sarpkaya, T., "In-Line and Transverse Forces on Smooth and Sand-Roughened Cylinders in Oscillatory Flow at High Reynolds Numbers," Technical Report No. NPS-69SL76062, Naval Postgraduate School, Monterey, California, 1976.

4. U. S. Senate Committee on Armed Services Preparedness Investigating Sub-Committee, "Inquiry into the Collapse of Texas Tower No. 4," 87th Congress, First Session, May 1961.

5. Naudascher, E. (Editor), Flow-Induced Structural Vibrations, Springer-Verlag, New York 1974.

6. Blevins, R. D., Flow-Induced Vibration, Van Nostrand Co., New York, 1977.

7. Sarpkaya, T., "Vortex-Induced Oscillations, A Selective Review," Journal of Applied Mechanics, Transactions of ASME, vol. 46, No. 2, pp. 241-258.

8. Laird, A. D. K., "Water Forces on Flexible Oscillating Cylinders," Journal of the Waterways, Harbors, and Coastal Engineering Division, ASCE, Vol 88, No. WW3, pp. 125-137, August 1962.

9. Vaicaitis, R., "Cross-Flow Response of Piles due to Ocean Waves," Journal of the Engineering Mechanics Division of ASCE, Vol. 102, No. EMI, pp. 121-134, 1976.

10. Selna, L. and Cho, D., "Resonant Response of Offshore Structures," Journal of the Waterways, Harbors, and Coastal Engineering Division, ASCE, Vol. 98, No. WWI, pp. 15-24, 1972.

11. Morison, J. R., O'Brien, M. P., Johnson, J. W., and Schaaf, S. A., "The Force Exerted by Surface Waves on Piles," Petroleum Transactions, AIME, Vol. 189, 1950.

12. Verley, R. L. P. and Every, M. J., "Wave Induced Vibrations of Flexible Cylinders," Proceedings of the Offshore Technology Conference, Paper No. 2899, May 1977.

13. McConnel, K. G. and Wilson, T. J., "Modelig Self-Excited Vibrations of Offshore Structures due to Wave Motion," Engineering Research Institute Report No. 77337, Iowa State University, May 1977.

14. Sarpkaya T., "Dynamic Response of Piles to Vortex Shedding in Oscillating Flows," Proceedings of the Offshore Technology Conference, Paper No. OTC-3647, May 1979.

15. Sawaragi, W. T., "Dynamic Behavior of a Circular Pile due to Eddy Shedding in Waves," Coastal Engineering in Japan, Vol. 20, 1977, pp. 109-120.

16. Thomson, W. T., Theory of Vibration with Applications, Prentice-Hall, Inc., Englewood, New Jersey, 1972.

17. Twigge-Molecey, C. F. M. and Baines, W. D., "Unsteady Pressure Distributions due to Vortex-Induced Vibration of a Triangular Cylinder," in Flow Induced Vibrations, Springer-Verlag, Berlin, 1974, pp. 433-442.

INITIAL DISTRIBUTION LIST

No. Copies

1. Defense Documentation Center   2
   Cameron Station
   Alexandria, Virginia   22314

2. Library, Code 0142   2
   Naval Postgraduate School
   Monterey, California   93940

3. Professor T. Sarpkaya, Code 69Sl   2
   Mechanical Engineering
   Naval Postgraduate School
   Monterey, California   93940

4. Department of Mechanical Engineering, Code 69   2
   Naval Postgraduate School
   Monterey, California   93940

5. Lieutenant Suleyman Ozkaynak   2
   Zeynepkamil Kartalbaba Sok.
   Feza Apartment No. 136/8
   Uskudar, Istanbul, Turkey

6. Dz. K. Komutanligi   2
   Egitim ve Kurslar Dairesi
   Bakanliklar, Ankara, Turkey

7. Istanbul Teknik Universitesi   1
   Makina Fakultesi
   Gumussuyu Cad.
   Istanbul, Turkey

8. Orta Dogu Teknik Universitesi   1
   Ankara, Turkey

9. Bogazici Universitesi   1
   Bebek, Istanbul, Turkey